(2)

Aquanautics
OxygenSystems

AD-A202 240

Final Report on the Artificial Gill Program

October 1987 - September 1988
Contract No. N00014-87-C-0335

Aquanautics Corporation
4560 Horton Street
Emeryville, CA 94608

October 28, 1988

Table of Contents

1. SUMMARY

This report summarizes the work carried out in the DARPA Phase IV program for the "Aquanautics Gill Technology" during the period from October 1, 1987 through September 30, 1988.

This report provides details of the three areas where major technological progress was achieved:

1. Carrier chemistry
2. Electrochemical carrier kinetics
3. Scale-up and cell improvements

The second and third areas of improvement led to a major reduction (more than 97%) in the size and cost for the production of a given quantity of oxygen at a given power.

The self-propelled demonstration vehicle was designed and most of the hardware procured. The testing of individual items was essentially completed. The highlight of the demonstration vehicle program was the small scale integration of the fuel cell and oxygen extraction unit (EOC). The integration process went very smoothly and all the design specifications were met. The fuel cell generated 18W and the EOC was operated at 4W. The power system demonstration with the gill in water was scheduled for September, 1988 and vehicle demonstration was scheduled for the next year.

In July, 1988, the focus of the program was expanded to include ocean-floor stationary power design. A conceptual design of the power system has been carried out. The design involves in-situ hydrogen generation from aluminum, oxygen extraction from seawater and direct feed of the Aquanautics carrier to a fuel cell. Keywords: fuel cells; power generation; oxygen generators; (KT)

System analysis for various types of power sources was also carried out to compare the gill system with stored oxygen systems. The system analysis shows that the gill system occupies much less volume and weighs less than the option involving stored oxygen. For example, a one kW-yr. unit delivering 1 kW power has the following weight and volume characteristics:

	Vol., l	Weight, kg
Gill System	3,000	6,000
Stored Oxygen	16,000	12,000
Li-Thionyl Chloride Battery	14,000	20,000

2. AQUANAUTICS OXYGEN EXTRACTION TECHNOLOGY

Aquanautics Corporation has developed a novel technique for separating oxygen from feed sources using regenerative oxygen binding organometallic compounds (carriers). In this proprietary process an electrochemical cell is used to oxidize and reduce the organometallic carrier complex. As shown schematically in Figure 1, an oxygen carrier acts like a circulating hopper that picks up and unloads oxygen in response to the application of an electrochemical voltage.

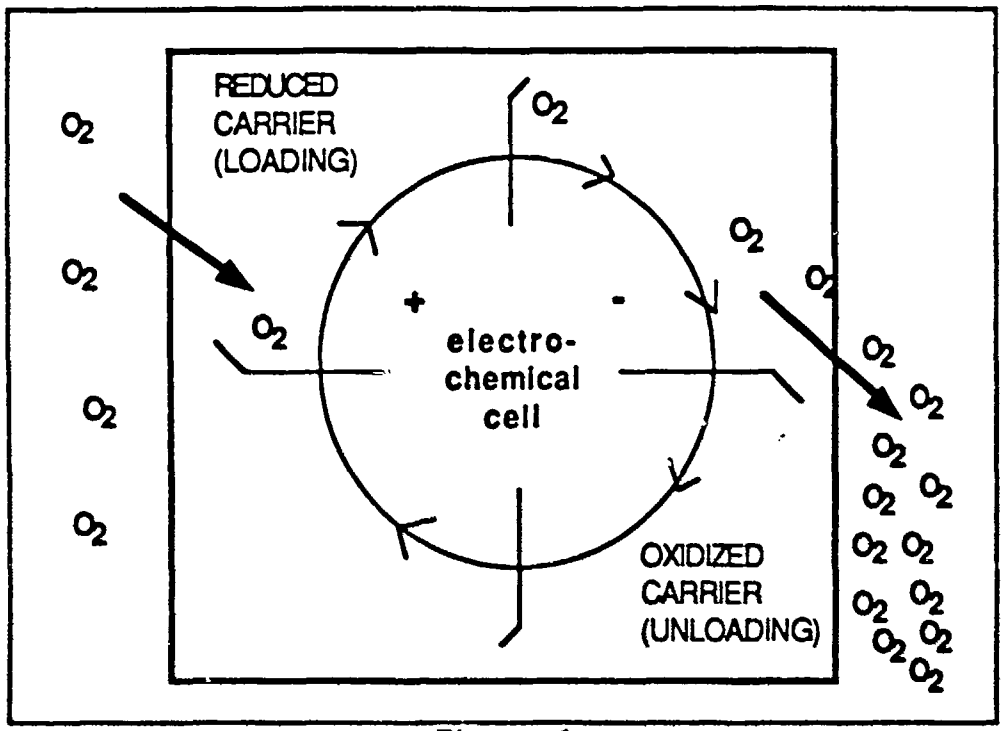

Figure 1

In its reduced state, an oxygen carrier has a natural affinity for oxygen. By circulating the carrier into an electrochemical cell and applying a voltage, the carrier oxidizes to a stable oxidized state and does not bind oxygen. This step results in oxygen desorption. When the carrier is regenerated through electrochemical reduction it is ready to bind oxygen again when brought into contact with the feed stream. The highly reversible nature of the electrochemical regeneration process results in substantially reduced energy consumption relative to temperature or pressure swing techniques. Laboratory research indicates that electrochemical regeneration could require less than half of the energy required for gaseous separation by conventional means. These laboratory scale experiments have been scaled up to produce over approximately three hundred milliliters of oxygen per minute without scaling difficulties. It is anticipated that systems can be scaled linearly to any desired output level. This economical and easily scaled process represents a breakthrough in separation technology. The circulating carrier oxygen separation system can be divided into four components illustrated by Figure 2 and explained below. The design of each component is specific to the nature of the particular application.

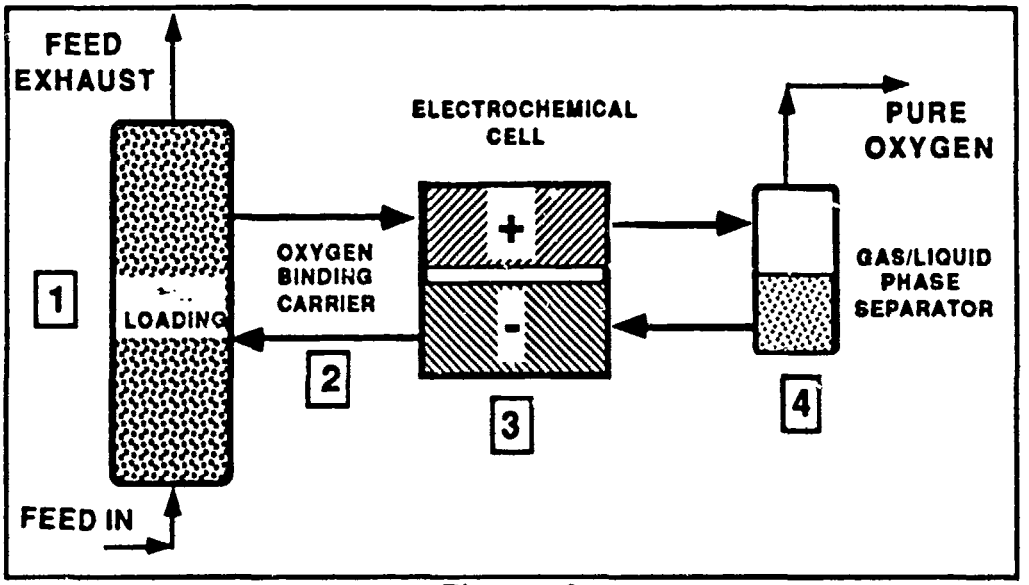

Figure 2

1. **The Loading Module.** The purpose of this component is to contact the feed with the carrier fluid. Aquanautics currently employs microporous hollow fiber polymer membranes as loading modules. Oxygen is driven through the membrane pores by the oxygen partial pressure gradient between the seawater stream on one side of the membrane and the carrier solution (which is, by definition, at an oxygen partial pressure of zero) on the other. While such membranes are only one of several options for loading from gaseous feeds, they are essential to underwater or liquid feed applications since the membrane prevents the mixing of the liquid feed with the carrier fluid.

2. **The Proprietary Carrier Fluid.** This component is the media which binds, concentrates, and releases oxygen and is the basis for selective oxygen extraction over other gaseous elements. The oxygen carrier is a transition metal compound whose valence state can be reversibly cycled. A pump circulates this fluid through the loader, cell anode, unloader, cell cathode, and back to the loader.

3. **The Electrochemical Cell.** This component is responsible for redox modulation of the carrier fluid. The anode of the cell is the site for oxygen desorption. After passing through the unloader, the cathode reduces the complex which restores oxygen affinity. The most common configuration is one where the anode and cathode are juxtaposed.

4. **The Unloader.** This final component is responsible for separating the gaseous oxygen resulting from electrochemical desorption from the liquid carrier.

3. TECHNOLOGICAL PROGRESS

There has been major technological progress in three areas of the Aquanautics oxygen extraction system. They are:

1. Carrier chemistry
2. Carrier electrochemical kinetics
3. Scale-up and cell improvements

This progress has led to:

1. Improved method of carrier characterization for future study.
2. Improved cell performance in power, size and cost to produce a given quantity of oxygen per unit time; to produce 1 lpm of oxygen at 100W/power level, the Aquanautics system would have required 10 ft^3 of cell volume and would have cost $400,000 a year ago. This can be accomplished by 1/3 ft^3 of cell volume and $6,000 today.

Details of this progress follows.

3A. CARRIER CHEMISTRY

SUMMARY

In the past year Aquanautics Corporation has developed a method for studying oxygen carrier compounds. It is now possible for Aquanautics to design new compounds and to predict their oxygen affinity. The lifetime of these compounds has been shown to vary from an hour to 27 days in static tests. Similarly, lifetimes have been and are continuing to increase in the EOC system. As yet, a solid structure/function relationship covering carrier lifetime has yet to be developed. However, the necessary data is rapidly being accumulated. Such a relationship should be formulated in the forthcoming year.

INTRODUCTION

Aquanautics Corporation has established a systematic process for evaluating oxygen carrying compounds. This process has been optimized to produce data on power consumption and longevity in the relatively short time of two (2) weeks. Over seventy (70) compounds have been synthesized and ten are being synthesized by Aquanautics or its sub-contractors. All but seventeen of these compounds have undergone an initial pre-screen designed to immediately eliminate those compounds that do not bind oxygen. (Eighteen have been eliminated to date.) The screening process includes the determination of carrier protonation, metal binding, and oxygen affinity constants. Further, the electrochemical behavior of the carriers is determined by cyclic voltammetry and coulometry. From this data, a reasonable estimate of carrier performance can be formulated.

Recently, Aquanautics has changed the screening process to include carrier longevity. In the past year the power to extract a liter of oxygen has been minimized while optimizing the output. However, this system was effective for only a few days. In order to produce a viable oxygen extraction system, a

longer-lived carrier is required. Thus, experiments designed to address longevity are routinely included in the screening process. This has lead to an increase in system lifetime to up to 40 days.

In parallel with this work has been the development of a mathematical model of the oxygen extraction system. This rather simple thermodynamic model has successfully predicted the observed trends in power and electron efficiency of the oxygen extraction process. The following report describes the progress made in the past year. However, due to the proprietary nature of most of this work, specific compounds and certain numerical results will not be listed, except in a general or qualitative sense.

EXPERIMENTAL

Determination of protonation, metal binding, and oxygen affinity constants. The potentiometric titration method was used[1]. A. A 15 ml. aliquote of a 1.5 mM solution of the ligand hydrochloride salt was placed in a sealed water jacketed beaker. The beaker was equipped with a stir bar, inert gas inlet, pH probe, and a titration burett. The vessel was maintained at 25 $\pm 0.1^{\circ}C$ throughout the titration. The ligand solution and the standard 0.01N potassium hydroxide titrant were both made with 0.1M KCl in order to maintain constant ionic strength. Addition of titrant and pH measurement was accomplished with a Mitsubishi Model GT-05 auto titrator for the protonation and oxygenation constant. A $\Delta pH/\Delta t$ of 0.005 pH unit/sec had to be obtained before the next increment of base was added. When the oxygen affinity was to be determined the inert gas inlet was changed to either air or oxygen.

The metal binding constant determination required completely O_2 free solutions. Since teflon tubing was used in the auto titrator, it was not possible to guarantee deoxygenated conditions. In these cases, a normal 10 mL glass burett equipped with a inert gas inlet was used. The pH measurements were obtained with a Cole-Palmer Model 5985-80 pH meter. Either a pencil epoxy body combination or glass combination pH electrodes were used.

Three titrations are required to obtain the various constants. First, only the ligand hydrochloride is titrated to obtain the protonation constants. The titration is then repeated with one equivalent of cobalt(II)chloride added under inert and oxygen atmospheres to obtain the metal binding and oxygen affinities, respectively.

The desired constants were extracted from the data by a curve fitting routine developed by Motekaitis and Martell[2,3]. A typical set of titration curves is shown in Figure 3.

---

[1]Rossotti, F. C. and Rossotti, H. S. The Determination of Stability Constants, MaGraw-Hill, New Youk, 1961.

[2]Motekaitis, R. J. and Martell, A. E. *Can. J. Chem.* 1982, *60*, 168-173.

[3]Motekaitis, R. J. and Martell, A. E. *Can. J. Chem.* 1982, *60*, 2403-2409.

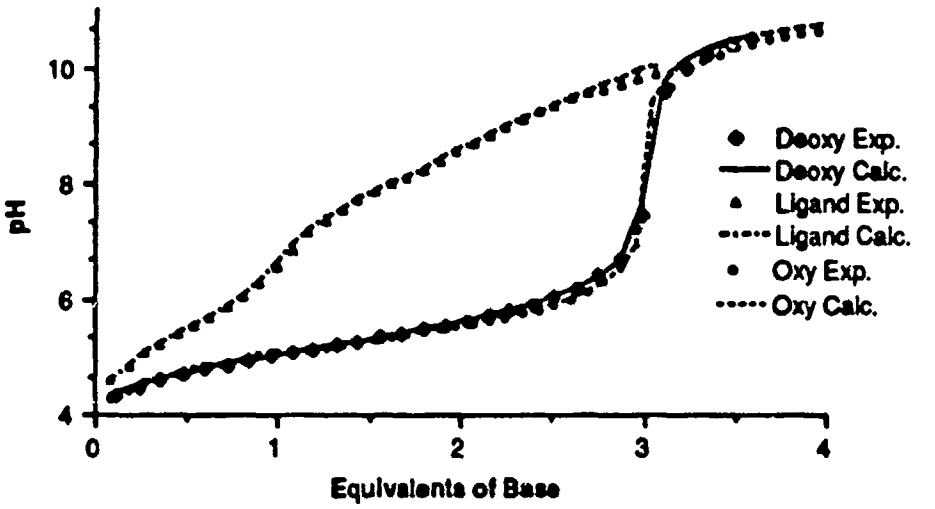

Figure 3. A typical set of titration curves for an oxygen carrier. The ligand protonation constants are determined from the Ligand Experimental points Metal binding constants use the Deoxy Experimental points and the oxygen affinity constants are determined from the Oxy Experimental points.

Cyclic Voltammetry. Cyclic voltammograms were obtained on 1-4 mM solutions of the ligand/metal complex. Potassium chloride at 0.5 or 1.0 M concentration was used as the supporting electrolyte. Either a BAS model CV-1B or CV-27 potentiostats were used to obtain the voltammograms. Voltammograms on both the deoxygenated and oxygenated complex were obtained. The pH used was that at the endpoint obtained from the potentiometric titration of the complex under oxygen. In some cases, the CV of the oxygenated complex was obtained at several different pH values.

A three-electrode system consisting of a Ag/AgCl reference, a platinum wire auxiliary, and either a glassy carbon or gold button working electrode, was used.

Coulometry. Coulometry was obtained in a two-compartment electrochemical cell separated by a TFI cationic exchange membrane (RAI). The working compartment utilized a carbon felt electrode and Ag/AgCl reference. The auxiliary compartment used a carbon sponge electrode and was filled with ca. 10 mM ferricyanide solution. The working compartment was filled with ca. 10mL of 4 mM carrier-O_2 complex. A YSI Clarke type oxygen electrode was inserted into the carrier solution.

Initially, the applied potential to the carbon felt was increased positively in steps until a reasonable rate of oxygen evolution and current flow were observed. The cell was held at that potential until 1 coulomb of charge had past through it.. A more negative potential was then applied in order to re-

reduce the complex. Air was bubbled through the solution to re-oxygenate it. The oxidation cycle was then repeated several times. The results were reported in terms of the rate of O_2 evolved, the oxidation and reduction potentials, the ΔE, and the current flow. Carriers with small ΔE, low oxidation potential, and fast O_2 evolution were desired.

RESULTS AND DISCUSSION

Oxygen Affinity. The oxygen affinity and metal binding constants have been determined for 21 compounds. The oxygen affinities vary from 2.5×10^5 to 1.6×10^{12}, spanning nearly 7 orders of magnitude. A structure/function relationship between the carbon chain length and the log K^{O2} has been proposed. It has been observed that the oxygen affinity decreases as the chain length increases. A similar trend was observed for the metal binding constants. Thus, it is now possible to design compounds and predict with fair accuracy the oxygen affinity, within a homologous series.

A study of the energy (1/wavelength) of the charge-transfer UV-visible absorbtion band and the oxygen affinity revealed a linear relationship for one homologous series. A plot of 1/Lamda vs. log K^{O2} is shown in Figure 4. Such relationships may allow the rapid determination of the oxygen affinity by simply obtaining the UV-vis spectrum of the compound. This study is still continuing in order to determine how general it is.

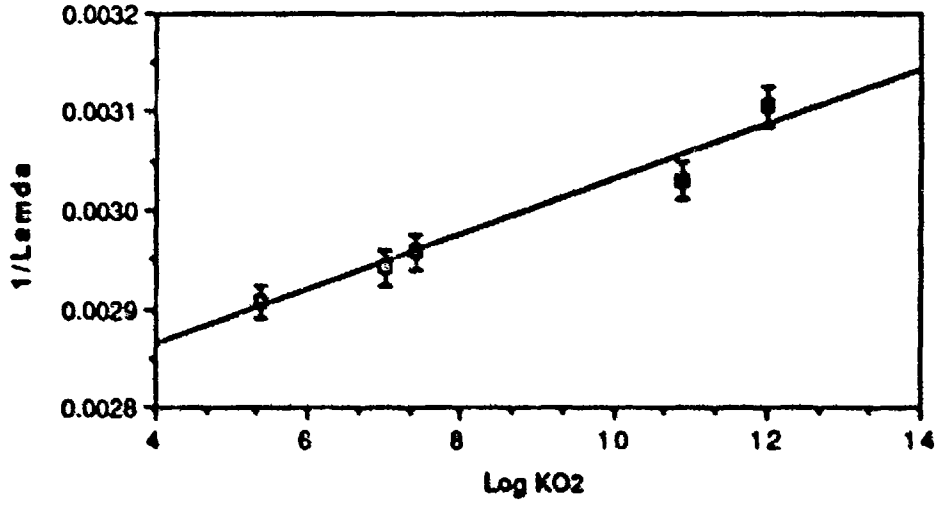

Figure 4. The linear relationship between the energy of the Metal-Oxygen charge transfer band and the oxygen affinity.

Coulometry. The coulometry experiment represents the smallest model of an operating EOC system that has been developed by Aquanautics. Two very

significant pieces of information are obtained from this work. The first is the potential required to oxidize the complex and release oxygen. The second piece of information concerns whether the carrier can be reduced back to its active oxygen binding form. If a candidate complex fails at either one of these, it can be excluded from further work in an EOC prototype unit. The performance can be summarized by comparing the cell potential, ΔE (the difference between the oxidation and reduction potentials) and the rate at which oxygen is released. This later value can be estimated by following the time response of the oxygen probe at a constant applied potential. The method is not accurate, but does allow one to make qualitative comparisons. Figure 5 shows the ΔE and O_2 evolution rates for a series of compounds. The class designations in Figure 5 refer to compounds that contain either pyridine or imidazole groups in their structure.

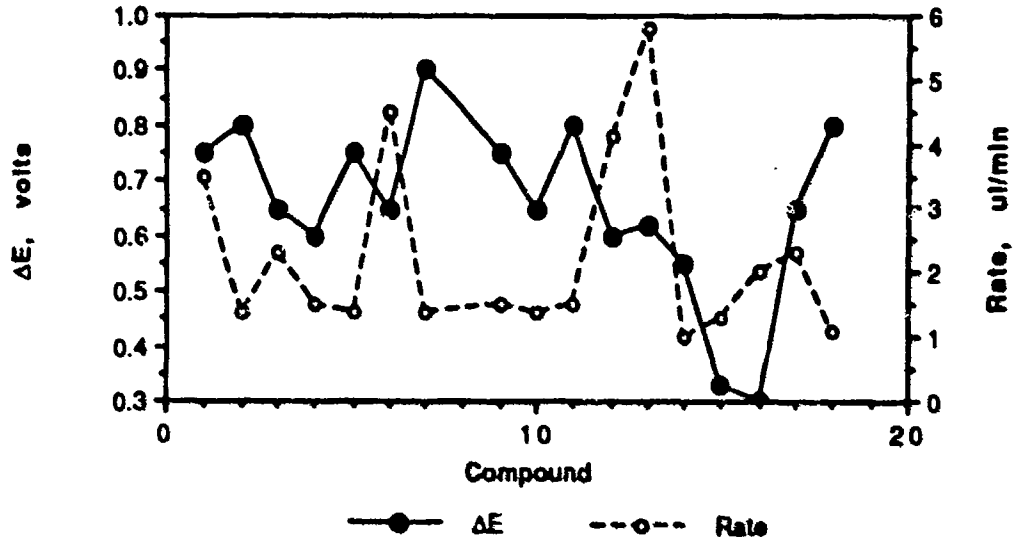

Figure 5. Variation of the ΔE and Oxygen evolution rate for several compounds.

It is possible to lower the ΔE required by adding an electrochemical catalyst. Such a catalyst undergoes oxidation and reduction faster and at a potential lower than that observed for the oxygen carrier complex. The observed oxidation potential of the oxygen carrier is generally more positive than its thermodynamic potential, because of slow oxidation kinetics. Although the oxidation potential of the catalyst is lower than that observed for the carrier, it is still greater than the carrier's thermodynamic potential. Thus, the catalyst can chemically oxidize the carrier. Under these conditions, the ΔE value is lowered and represents the difference between the catalyst's oxidation potential and the carrier's reduction potential. Several electrochemical catalysts have been investigated. The most promising one is routinely added to

the carrier solution undergoing coulometry to determine its catalytic efficiency. The results of adding a catalyst in the coulometric experiment are shown in Figure 6. The results indicate that a catalyst can significantly improve the electrochemical performance of the carrier. Interestingly, the uncatalyzed results show that while ΔE does not change much from compound to compound, the oxygen evolution rate can vary by a factor of 5.

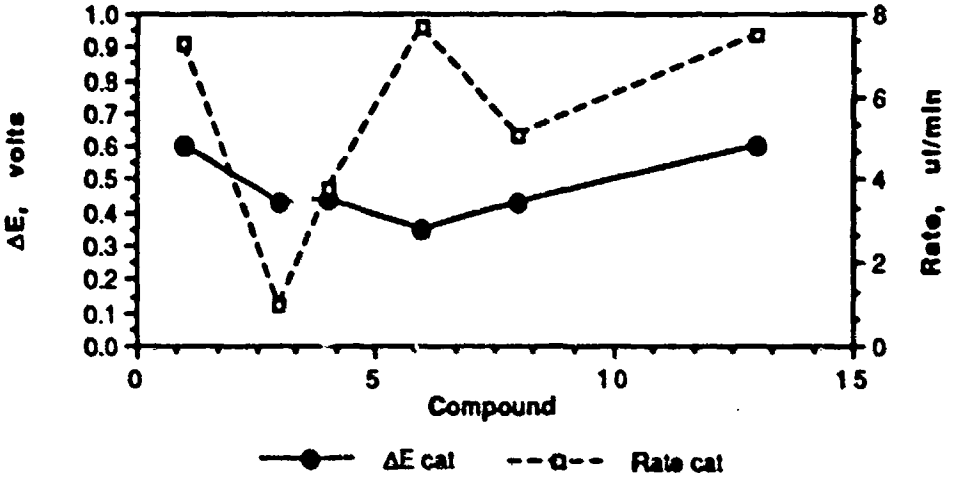

Figure 6. Same as Figure 5 except that an electrochemical catalysis was added. Only a few of the compounds in Figure 5 have been catalyzed.

Lifetime. The carrier half-life has been measured spectroscopically by monitoring the disappearance of the cobalt-oxygen charge transfer band. This method has the advantage of being simple, rapid, and requiring milligram quantities. A correlation between the spectroscopic and EOC lifetimes has been observed in a few cases. A definite trend has not yet been established. Interpretation of the results is not straightforward. In some cases, the initial decomposition product can again bind oxygen and the resulting complex can decompose again. It has not been possible to identify the intermediate species.

However, with the eleven compounds studied, a half-life range from 17 minutes to 27 days has been observed. The workhorse carrier, 33-SuzyP, which lasts for 3 days in an EOC, has the relatively short spectroscopic half-life of 1.4 h. A similar compound with a half-life of 17 h has lasted 40 days in an EOC. Since other carriers have even longer half-lives, it is expected that an EOC operating for more than forty days is possible.

Mathematical Modeling. Using a simple thermodynamic model, based on Eq. 1, it was possible to calculate the energy required to generate a liter of oxygen. This power varied directly with the log K_{O_2} value at high oxygen affinities and inversely at low oxygen affinities. The energy increased for all

oxygen affinities as the fraction of oxy complex (fractional conversion) which released oxygen increased (see Figure 7). Further analysis of this data resulted in the determination of the number of electrons required per oxygen released.

$$\Delta G = \Delta G^{0} + RT \ln \left(\frac{[\text{oxy complex}]}{[\text{deoxy complex}]^{2} [O_2]} \right) \qquad \text{Eq. 1}$$

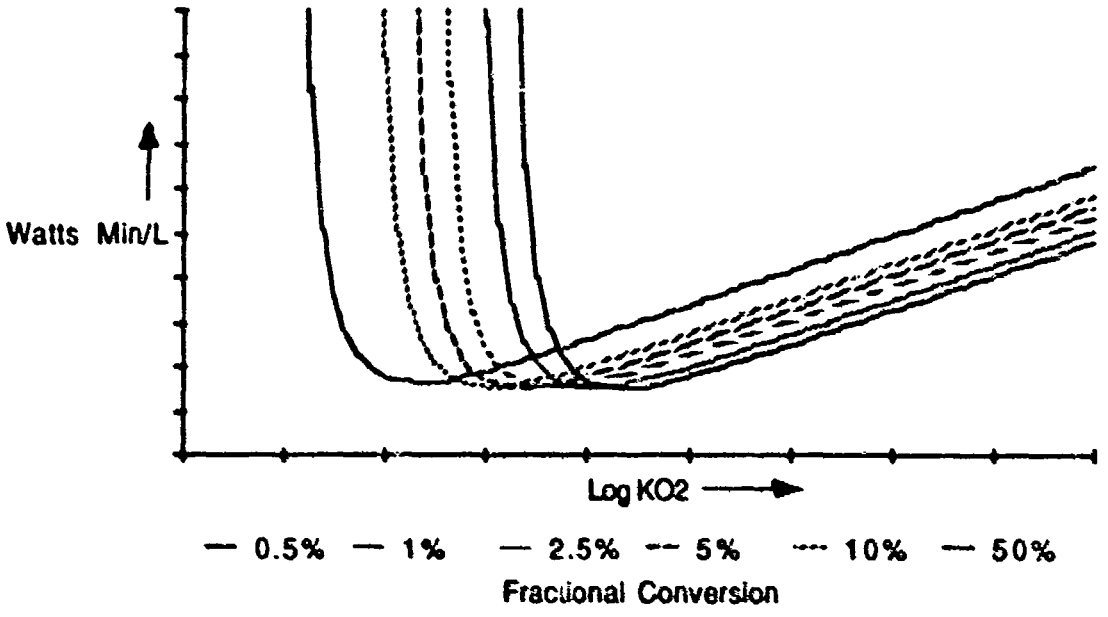

Figure 7. The power to generate a liter of oxygen at 1 atm. as a function of the oxygen affinity and fractional conversion.

The number of electrons required per oxygen molecule released is called the electron count. This electron count assumes an electrochemical process, defined in Scheme 1.

$$LMO_2ML \Longleftrightarrow 2LM^{+} + O_2 + 2e^{-}$$

$$2e + 2LM^{+} \Longleftrightarrow 2LM$$

$$2LM + O_2 \Longleftrightarrow LMO_2ML$$

Scheme 1

Note that under the best conditions, the electron count cannot be lower than 2. It was found that the electron count paralleled the energy required. At high oxygen affinity its value was 2 and at low oxygen affinity it increased (Figure 8).

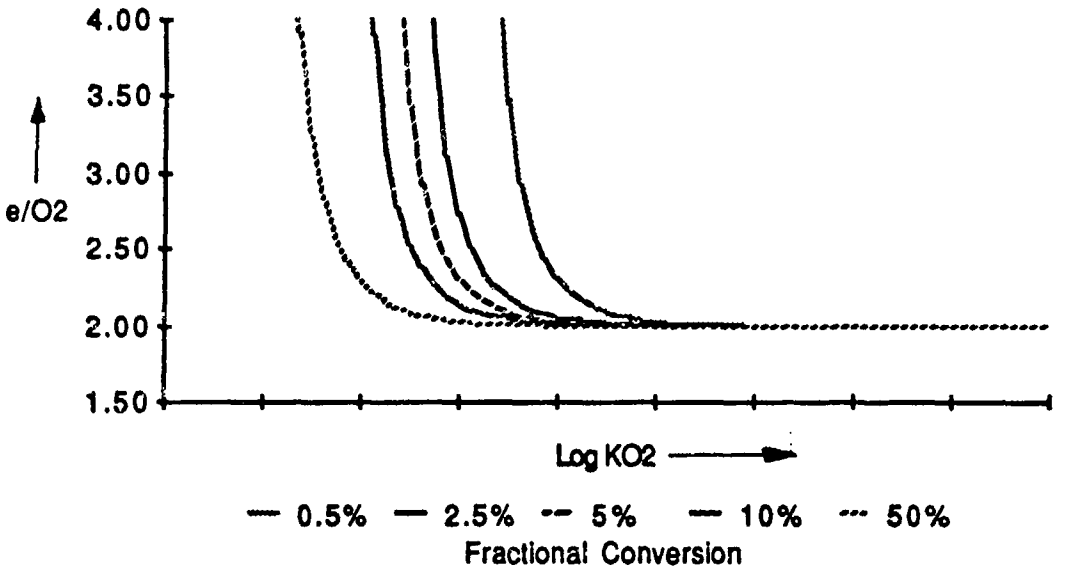

Figure 8. The variation of the electron count as a function of the oxygen affinity and fractional conversion.

The model has thus allowed the optimum conditions for low energy oxygen production to be determined. This determination takes into account the initial oxygen pressure, the delivered (final) oxygen pressure, temperature, carrier concentration, and fractional conversion. The predictions made using the model compared well with EOC data. Thus, a rather complicated chemical system was successfully modeled with a simple equation.

3B. CARRIER KINETICS

The overall objective for carrier kinetic research during 1988 was to provide a fluid and electrode system capable of delivering a minimum oxygen production density of 1.5 l/min/m^2 of electrode area at a cost of 100 watts/liter O_2/min. by using readily available carriers with at least 24 hour lifetime. This output level and power for oxygen production was obtained from a parametric model detailing the energy needs of a self-propelled demonstration vehicle. However, while such power and output are sufficient for a demonstration, the ultimate goal of 6 l O_2/min/m^2 at 40 watts/Liter/min. was set as the level needed for a practical oxygen extractor with a carrier lifetime of several months. The major highlight for this year is the achievement of an oxygen output density of 2.0 l O_2/min/m^2 requiring only 50 watts/liter/minute. These results are summarized in Figure 9. The electrode area required yields the volume of the cell when cell thickness and packaging efficiency of electrodes are known. Therefore, the x-axis in Figure 9 is inversely proportional to the required volume of the cell to produce 1 lpm of oxygen.

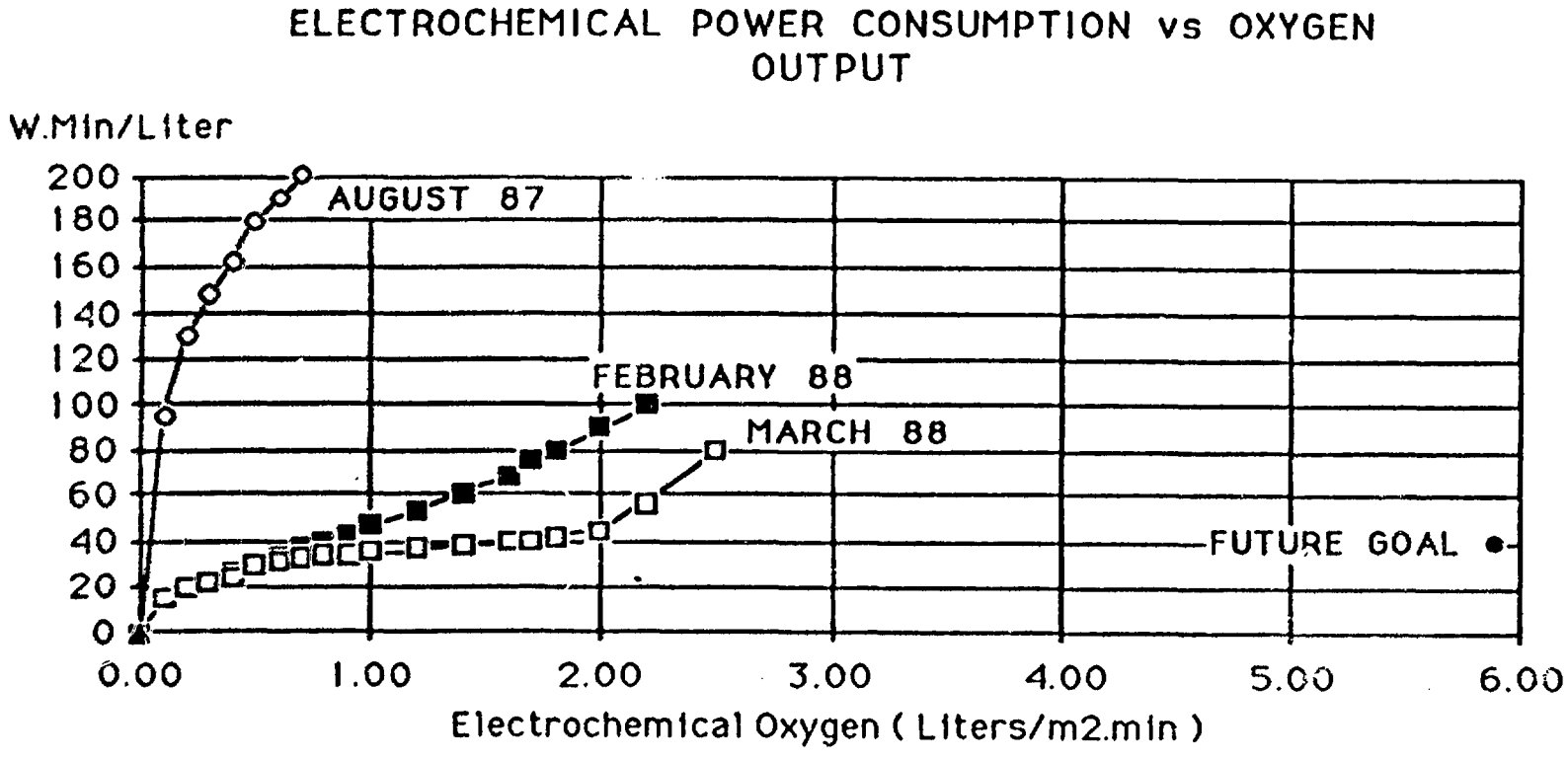
ELECTROCHEMICAL POWER CONSUMPTION vs OXYGEN OUTPUT
W.Min/Liter
200
180
160
140
120
100
80
60
40
20
0
AUGUST 87
FEBRUARY 88
MARCH 88
FUTURE GOAL
0.00
1.00
2.00
3.00
4.00
5.00
6.00
Electrochemical Oxygen (Liters/m2.min)

Fig. 9

$$\text{Occupied Cell Volume} = \frac{t \times p \times q}{x}$$

where
- t = cell thickness, m
- p = packing efficiency, m^2/m^3
- q = liter of oxygen/min.
- x = liter/min/m^2 (x axis in Figure 9)

Such gains in oxygen output and decrease in power can be attributed to several areas of research spanning engineering, carrier, and materials research. One highlight in carrier kinetic research was the elucidation of the rate-limiting step for oxygen release when employing the benchmark carrier. This knowledge made possible the selection of an effective electrocatalyst which was introduced routinely into the carrier solutions. The use of such catalyst in conjunction with the improvements made in the cell, such as choice of separator, increased conductivity of the solutions and contact losses led to the enhancements in the power and output performance of the carrier. Previously unsuccessful experiments with other catalysts and other carriers led to an understanding of the requirements for the catalyst with respect to its ability to catalyze oxygen release, to be stable and to be inert towards the carrier itself so that it only facilitated the desired reaction. Another highlight for the year came from an electrode materials program. The rate of electron transfer with oxygen carriers can be dependent only only on the kind of electrode (for example carbon, gold, or platinum), but in the case of carbon, the nature of the carbon surface as well

Additionally, this year saw the beginning of research to provide data for cell and process modeling. Preliminary experiments were performed providing exchange current densities (Tafel plots) on the carrier and electrocatalyst at various electrode materials. Diffusion coefficients for various carriers were also determined. Finally, a method for cleaning the electrochemical cells without disassembling them was developed. This method has been incorporated in all routine system experiments and has reduced set-up time dramatically.

The latter part of this year has been dedicated to working on more sophisticated techniques to obtain kinetic data. Since the ultimate goal of oxygen output and power will require better-performing carriers, more detailed knowledge, based on improved cell and mechanistic models, are being developed. A major question which still remains to be resolved is the determination of the slow electrode. When the program was first begun there was no doubt that the slow electrode was the anode but now both electrodes are in balance and for some new carriers there is evidence that the cathode reaction is the rate-determining process. It is therefore likely that another catalyst will be required to facilitate the cathode reaction.

The work carried out with the benchmark carrier demonstrated that the performance had been pushed to the limits of the carrier's capability. Further improvements require new carriers to be studied, as it appears that the performance is a function of the carrier structure. The benchmark carrier also suffered from severe lifetime problems which limited its usefulness to a

demonstration vehicle. Thus a new program has been initiated to study the lifetimes of a range of carriers in the EOC apparatii. Concurrently, the kinetics of these carriers will be evaluated to determine the structural features which facilitate the oxygen release process. The goal of the program then is to find a carrier with at least a three month lifetime and with kinetics capable of allowing the power and output goals to be attained.

For this purpose Aquanautics is increasing its EOC capability by installing 4 new apparatii to screen carriers for lifetime and kinetics. Further simplified systems will be installed in the next year to allow cost-effective screening of carrier performance lasting several months. Already a carrier has been discovered which has an effective lifetime of greater than one month although its power requirements are higher than those of the benchmark carrier. Arrangements for custom synthesis of several new families of carriers have been made which will allow a systematic study of the lifetime and kinetics to be made. The initial screening process for these compounds is described in Section 3A. The carriers which show promise from the initial screening are then examined in an EOC and if they show sufficient grounds for optimism enough material is then synthesized to allow several long term runs to be made. From this a new benchmark carrier will emerge to allow underwater applications to emerge.

This process of evaluation has been shown to be very necessary from two points of view. The first is the obvious one of lifetime. The second however was peculiar to the underwater gill. Due to the nature of the gill membrane it was found to be necessary to reduce the salt content of the carrier electrolyte in order to equalize the water vapor pressures inside and outside the membrane. This led to a large increase in the resistance of the solution and to an increase in the power requirement. The only way around this problem is to reduce the gap between the electrodes and this implies the need for flat plate electrodes or high surface area electrodes with low volume requirements. For such a design to be practical the carrier kinetics would require to be at least an order of magnitude higher than those obtained at present. The search for new carriers thus has a great impact on the design options available and indeed on the possible applications of the technology.

3C. SCALE-UP AND CELL IMPROVEMENTS

From the laboratory studies, it was determined that about 7,500 cm^2 of the electrode area of the cell will be needed for the vehicle. In this program, scale-up of the oxygen extraction system from bench size to demo-vehicle scale was carried out. Major effort was expended in the area of cell design because:

1. They are the most expensive components of the system, and
2. They occupy a large volume in the vehicle.

In the area of cell design , scale up was carried out from a 25 cm^2 (bench size) to a 100 cm^2 cell size. The 100 cm^2 cell is commercially available from Electrocell AB of Sweden and is known as the MP Cell.

All the improvements carried out on the bench scale system were verified in the larger of cell. The progressive improvement in the technology is shown in Figure 10. Here the energy required per unit volume of oxygen is plotted against the oxygen evolution rate per unit area of electrode.

The improvements were:

1. Increase of conductivity
2. Optimization: Choosing the right concentration of carrier and carrier flow rate.
3. Catalyst: Introduction of a catalyst in the carrier.
4. Choice of separator

Unfortunately, increased conductivity could not be utilized in this case because of water ingress from seawater to the carrier through the gill due to vapor pressure differences.

Aquanautics also engaged in the design of its own cell because of the following drawbacks of the commercially available MP cells:

1. They are quite expensive at $\$80,000/m^2$.
2. Packaging efficiency ($9\ m^2/m^3$).was small leading to large cell volume.
3. The cells could not be used as a bipolar stack without losing efficiency.

As related to the third reason, a 20% drop of output was observed in an experiment when 5 MP cells were stacked in bipolar mode. A monopolar mode requires low voltage and high amperage. A fuel cell stack normally provides 12V whereas a single oxygen producing cell operates at around 0.5V. This necessitates at least 24 Aquanautics cells assembled in bipolar mode. The reason for the MP cells' poor performance in a bipolar mode is thought to be due to shunt current that flows in the manifolds of the cells. MP cells have low electrolytic resistances in their manifolds[4]. The other option is to use a DC-DC converter with 10-20% power penalty.

[4]E.A. Kaminski and R.F. Savinell, "A Technique for Calculating Shunt Leakage and Cell Currents in Bipolar Stacks Having Divided or Undivided Cells", Journal of Electrochemical Society, 130, p. 1103-1107, 1983.

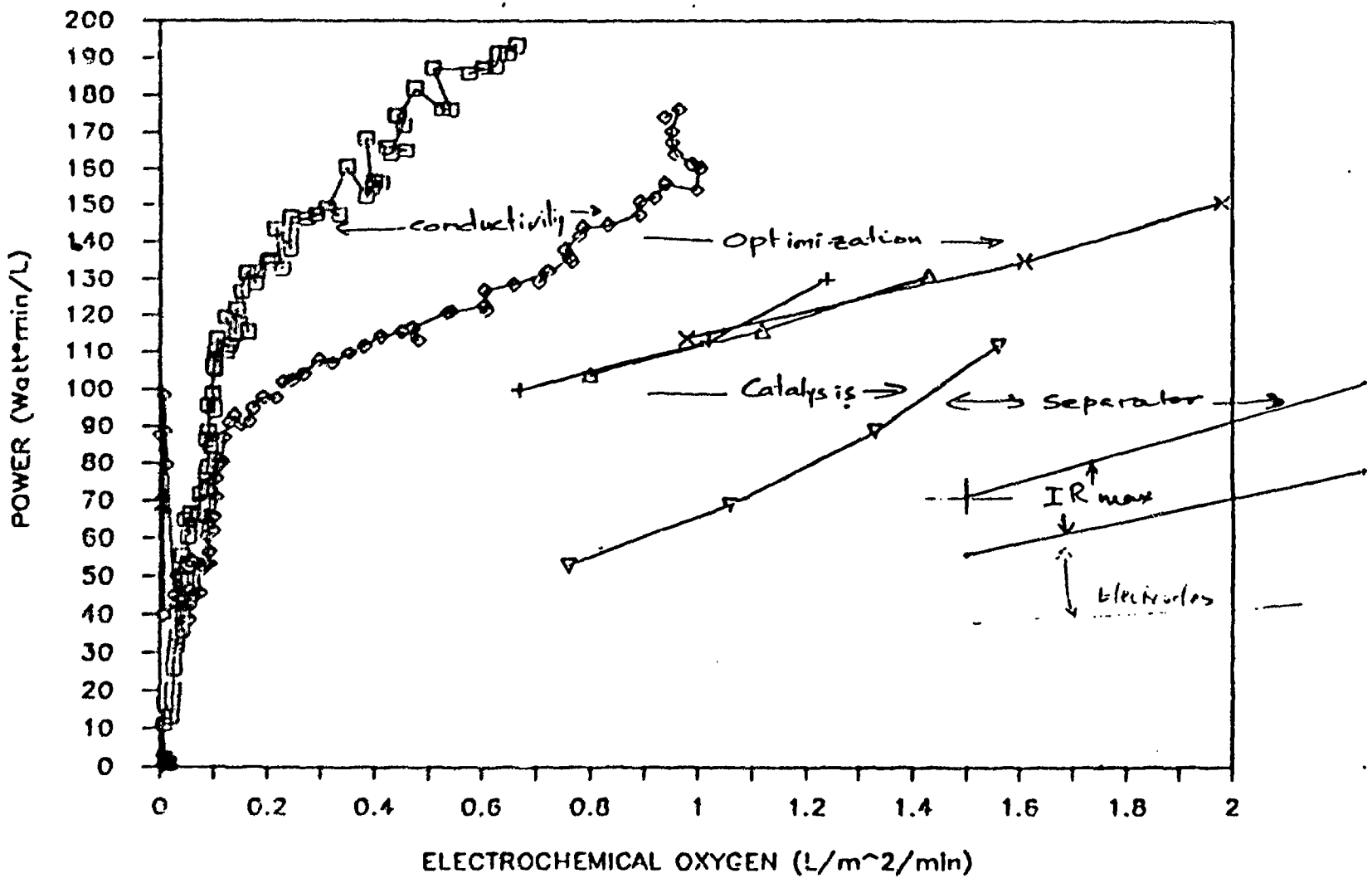

Fig. 10 (Progressive Improvement)

A comparison of the new cell design and the MP cell is:

	MP Cell	New Cell
Area/unit cell, cm^2	100	250
Packing Efficiency, m^2/m^3	9	25
Cost, $\$/m^2$	80,000	15,000
Efficiency, * Bipolar Mode	88%	98%

*Calculated according to Footnote 4.

4. ENGINEERING TOWARDS AUV DEMONSTRATION

Aquanautics' engineering team, with the help of Makai Ocean Engineering, worked towards a demonstration vehicle to prove that the concept of a gill-fuel cell to power a vehicle is a realistic proposition. The goal this year was to design a demonstration vehicle, procure most of the parts and demonstrate the excess power from a gill-fuel cell combination. The other aspect of the program was to develop an engineering and energy model. This model will be useful for future vehicle design.

The goal for the next year would have been to operate and demonstrate the vehicle and verify the model. In July of 1988, this AUV demonstration program was put on hold and the program was steered towards a stationary power system.

4A. CONCEPT

The concept of the AUV with a gill-fuel cell has been previously reported and a brief description follows.

The AUV design is shown in Figure 11. The major hardware components are:

1. Propulsion
2. Fuel Cell
3. Electrochemical Cell
4. Gill or Oxygen Loader
5. Seawater Filter
6. Seawater Pump
7. Hull

The design of the system was completed and most of the hardware components were procured. The smaller design was chosen as it was made possible after the technology improvement over the year. This design is about 5 times smaller than the larger model.

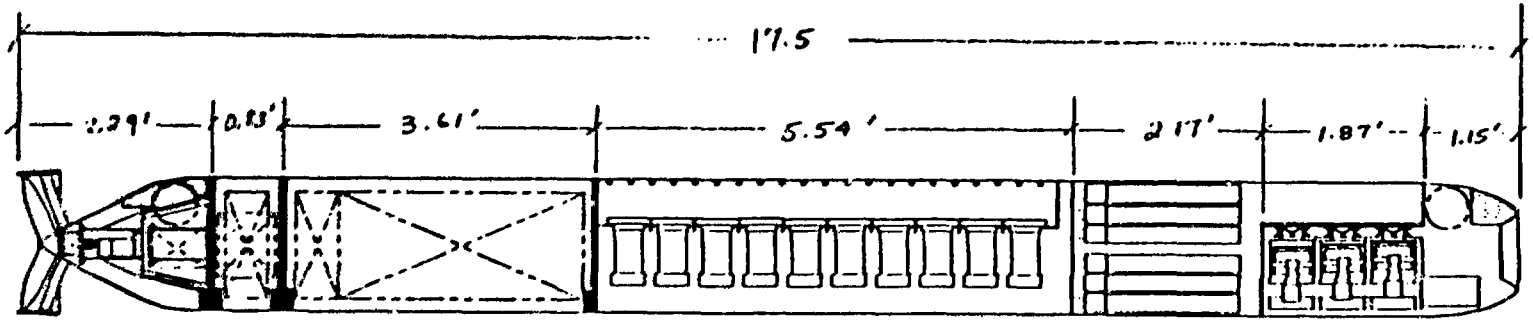

DESIGN SPEED = 0.5 KNOTS
LENGTH OVERALL = 17.5 '
OUTER DIAMETER = 20"

TOTAL POWER = 175 WATTS
O_2 REQ.: 0.44 LPM
POWERED BY: AL-O_2 F.C.

30 BARD CARTRIDGES
30 MP CELLS
DESIGN CONTINGENCY: 25%
ENDURANCE: 10 HOURS

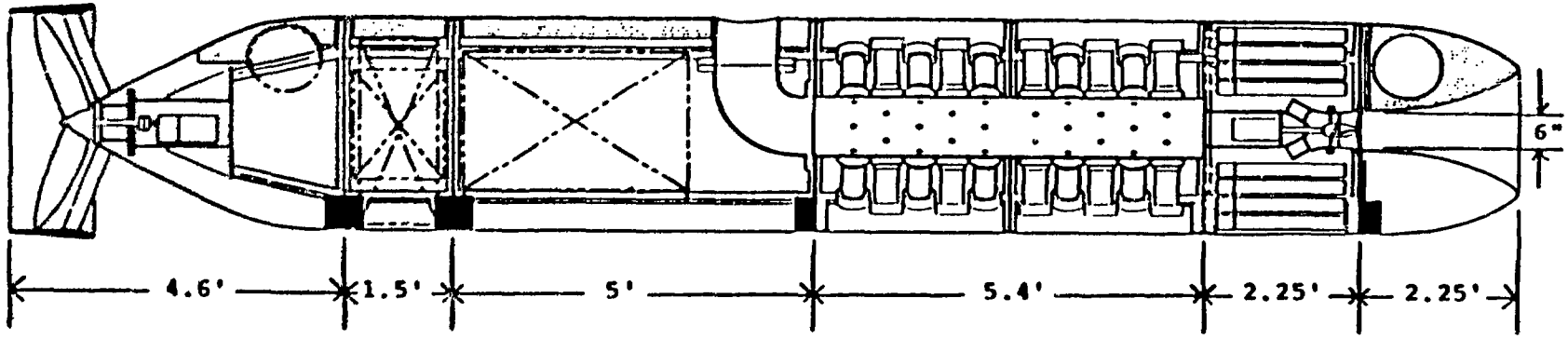

DESIGN SPEED = 0.5 KNOTS
LENGTH OVERALL = 21 '
OUTER DIAMETER = 39 "
VEHICLE DRY WEIGHT = 2987 pounds

TOTAL POWER: 300 WATTS
O_2 REQ'D: 0.748 LPM @ 25°C, 1 ATM
POWERED BY: AL-O_2 FUEL CELL
ENDURANCE: 10 HOURS

60 BARD CARTRIDGES
>70 MP CELLS
DESIGN CONTINGENCY: 12.5%

Fig. 11

4B. ENGINEERING MODEL

Prior to October 1987 Dale Jensen of Makai Ocean Engineering had devised a thorough and serviceable vehicle energy balance model which included several years worth of improvements and revisions. However, this model was concerned only with the power consumed by the electrochemical extraction system and not directly with the size of the system. It provided no goals for carrier development other than minimum specific power: watts per liter per minute of oxygen output.

In October of 1987 it was recognized that carrier pumping costs would be unacceptable if the carrier flow rates were scaled up. It was also noted that the cost of the electrochemical cell would be unacceptable at the output per unit separator area which were being achieved at the specific power levels called for by the energy balance model. These factors led to the formulation of two new subsystem models.

The first model predicted total specific power given carrier flow rate per unit of separator area and electrochemical power per unit of oxygen. Curves generated using this model allowed quick evaluation of the performance of a carrier and led to the adoption of experimental flow rates one quarter to one fifth of the previous flow rates. Figure 12 is a histogram generated by this model which yields the correction to the electrochemical specific power required as function of carrier flow rate and oxygen output.

The second subsystem model predicted the maximum excess power which could be generated by a given fuel cell, electrochemical oxygen cell and gill combination. Curves generated by this model, shown in Figure 13 give the system hardware required to produce 75 watts of excess power as a function of the carrier performance. These curves showed that the most important carrier performance characteristic for this system is the slope of the specific power versus output line and established performance goals for an economical system. (The curves also showed that the performance of the carriers being considered was such that more economical systems resulted from operating the carrier so as to maximize output rather than to minimize specific power.) The derivation of these carrier performance curves is discussed in the Appendix.

Figure 14 shows the output from the Makai energy balance model at the February 1988 design point and the corresponding power values from the August 1987 design point. The energy balance model reflects optimization done using the two previously described models as well as efforts to scale the vehicle down and progress in optimizing components. Cutting the vehicle diameter in half cut the gross propulsion power in half while maintaining the same vehicle velocity. The reduction in vehicle propulsion power and improvements in component performance resulted in a 42 percent reduction in total vehicle power. The major cost reduction in the February design resulted from reduction of the required number of electrochemical oxygen separation cells from more than 70 to less than 30 for a savings of more than $1000 per cell. Figure 15 summarizes the vehicle power system characteristics in a schematic form.

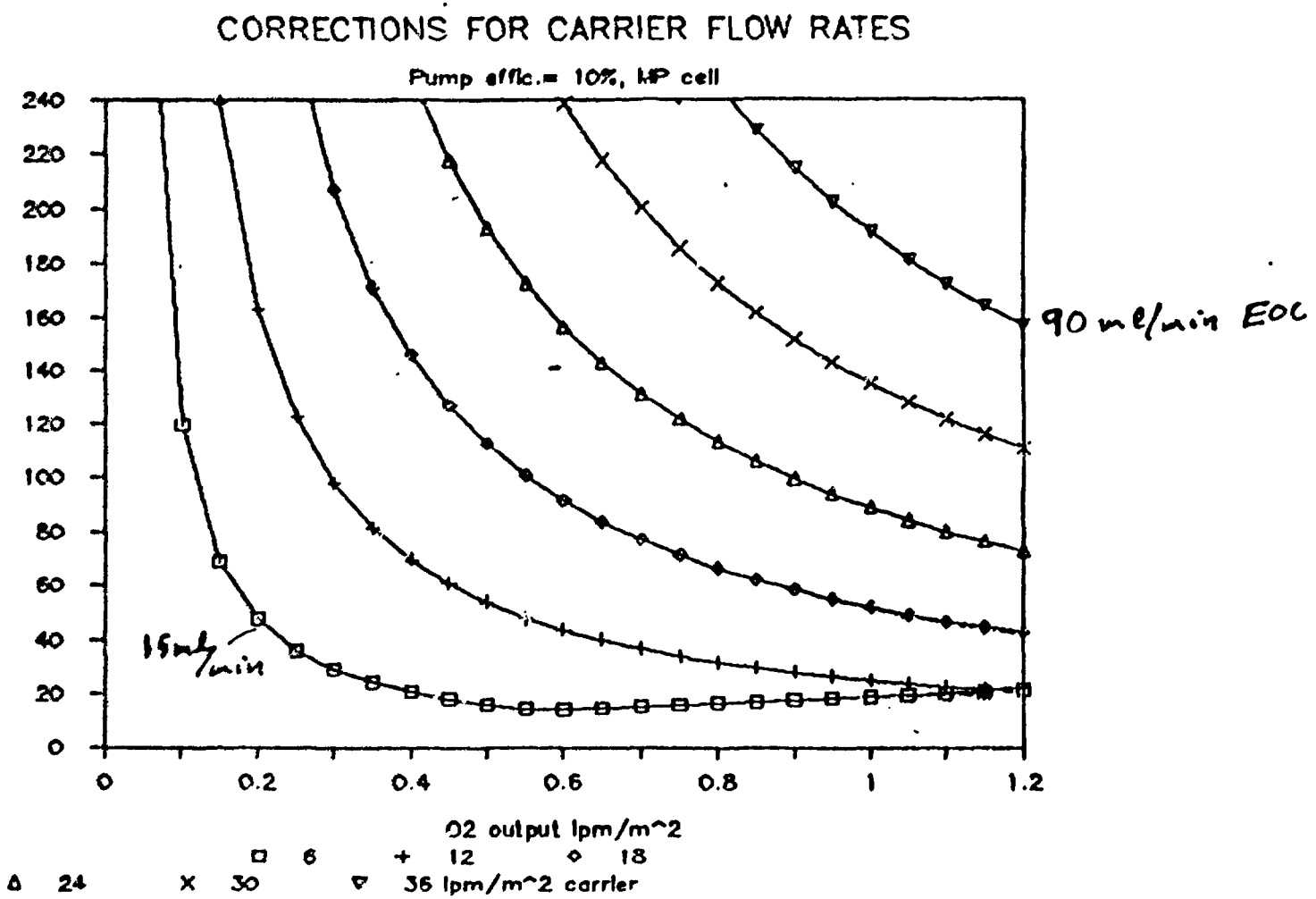
CORRECTIONS FOR CARRIER FLOW RATES
Pump effic.= 10%, MP cell
Add this to measured v*min/l
240
220
200
180
160
140
120
100
80
60
40
20
0
0
0.2
0.4
0.6
0.8
1
1.2
O2 output lpm/m^2
□ 6
+ 12
◇ 18
Δ 24
× 30
▽ 36 lpm/m^2 carrier
90 ml/min EOC
15 ml/min

Fig. 12

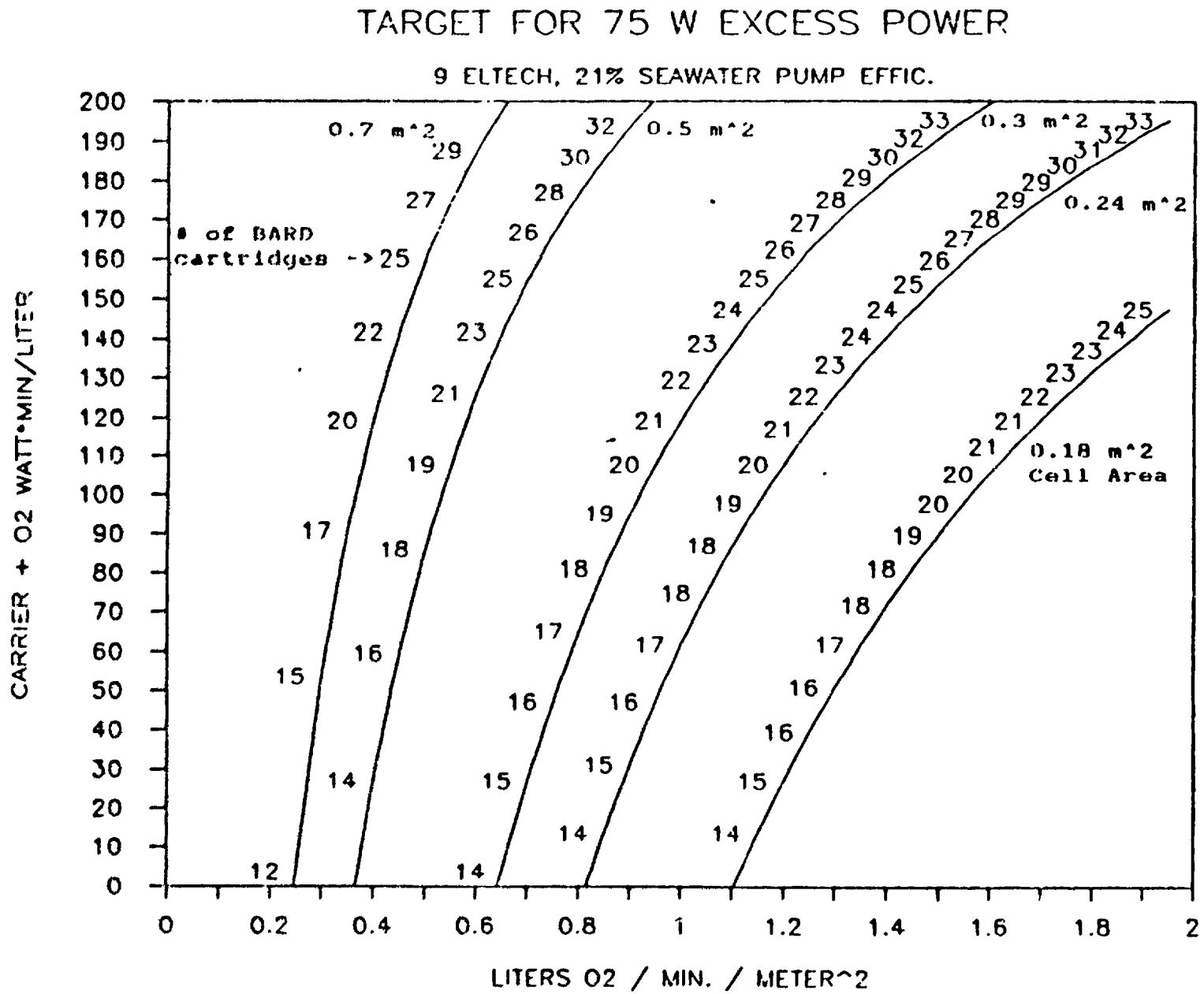
TARGET FOR 75 W EXCESS POWER
9 ELTECH, 21% SEAWATER PUMP EFFIC.
CARRIER + O2 WATT*MIN/LITER
LITERS O2 / MIN. / METER^2
# of BARD cartridges ->25
0.7 m^2
0.5 m^2
0.3 m^2
0.24 m^2
0.18 m^2 Cell Area
0
10
20
30
40
50
60
70
80
90
100
110
120
130
140
150
160
170
180
190
200
0
0.2
0.4
0.6
0.8
1
1.2
1.4
1.6
1.8
2

Fig. 13

ENERGY BALANCE, DARPA DEMONSTRATION VEHICLE 01-Feb-88 05:49 PM
AT CURRENT DESIGN POINT W/FLOW BY ELECTRODES IN HP CELL

			CURRENT POWER	CURRENT % OF TOTAL	AUGUST 87 POWER	AUGUST 87 % OF TO
AL-O2 FUEL CELL						
TOTAL OUTPUT			174 WATTS	100.0%	300 WATTS	100.0%
TOTAL EFFICIENCY	54.8	%				
> CURRENT EFFICIENCY	99.0	%				
VOLTAGE EFFICIENCY	55.3	%				
> FUEL CELL VOLTS/CELL	1.51	VOLTS				
> THEO. MAX CELL VOLTAGE	2.73	VOLTS				
OXYGEN REQ'D @ DEG C 25	0.442	LPM				
> FUEL CELL PARASITIC POWER	6.6	%	11 WATTS	6.6%	20 WATTS	6.7%
GAS CIRCUIT BLOWER						
> STOICHIOMETRIC FACTOR	2.15					
> PPO2 @ FC INLET	0.35	ATM				
GAS CIRCUIT FLOW	2.7	LPM				
> GAS CIRCUIT HEADLOSS	0.610	METERS FW				
> BLOWER EFF.	10	%				
BLOWER POWER			3 WATTS	1.5%	5 WATTS	1.7%
INSTRUMENTATION			2 WATTS	1.2%	2 WATTS	0.7%
OXYGEN EXTRACTOR						
PUMPING OF CARRIER FLUID			13 WATTS	7.3%	13 WATTS	4.3%
> O2 CONC LOADED IN CARRIERC	0.081666	L/L				
TOTAL CARRIER FLOW	5.4	LPM				
> NUMBER OF SERIES CART.	1					
CARRIER FLOW PER CARTRIDG	180.4	ML/MIN				
PUMP & MOTOR EFFICIENCY	10.0	%				
> PUMP CONTROLLER LOSSES	15.0	%	2 WATTS	1.1%	2 WATTS	0.7%
> # EC CELLS IN STACK	30					
HEAD LOSS	1.4	METERS FW				
> EOC POWER REQUIREMENT	102.0	W/(LPM)	45 WATTS	25.9%	97 WATTS	32.3%
GILL						
TOTAL AREA PROVD'D	133.3	M^2				
BARD CARTRIDGES	30.0	CARTRIDGES				
> GILL PACKING DENSITY	409.1	M^2/M^3				
OXYGEN PERMEABILITY	0.00046	LPS/(ATM-M^2)				
> INLET DIAMETER	0.20	M				
INLET AREA	0.03	M^2				
INLET VELOC (PIPE)	6.25	CM/SEC				
> OUTER DIAMETER	0.51	M				
FRONTAL AREA	0.20	M^2				
> BODY LENGTH	5.34	M				
O2 SOL IN SW @72 DEG F	0.024260	L/L/ATM O2				
> INLET O2 CONC IN SW	0.00508	L/L				
> OUTLET O2 CONC IN SW	0.00145	L/L				
SEAWATER O2 REMOVAL	71.46	%				
SEAWATER PUMPING			15 WATTS	8.9%	44 WATTS	14.7%
FLOW PER CARTRIDGE	4.1	LPM				
TOTAL FLOW	121.7	LPM				
> PUMP/MOTOR EFF	21.6	%				
60/60/60						
> PUMP CONTROLLER LOSSES	15.0	%	2 WATTS	1.3%	7 WATTS	2.3%
HEAD LOSS	0.164	METERS FW				
PROPULSION, GROSS			16 WATTS	9.4%	32 WATTS	10.7%
> SYSTEM CONTROLLER	15	WATTS	15 WATTS	8.6%	15 WATTS	5.0%
> MOTOR CONTROLLER LOSSES	15.0	%	2 WATTS	1.4%	5 WATTS	1.7%
> MOTOR	50.0	%				
> GEARS	50.0	%				
> PROPELLER	50.0	%				
NET PROPULSION POWER	2	WATTS				
FRONTAL DRAG FORCE	0.7	KG				
> FRONTAL DRAG COEFF	1.0					
SKIN FRIC DRAG FORCE	0.2	KG				
> SKIN FRIC COEFF(BODY)	0.006					
REYNOLD'S NUMBER (BODY)	109361					
> RESULTANT MINIMUM VEL	25.0	CM/SEC				
MAX VELOCITY POSSIBLE	30.3	CM/SEC				
> DESIGN CONTINGENCY	27%		46 WATTS	26.7%	58 WATTS	19.3%

Fig. 1B

DEMO VEHICLE EOC/POWER SYSTEM SCHEMATIC

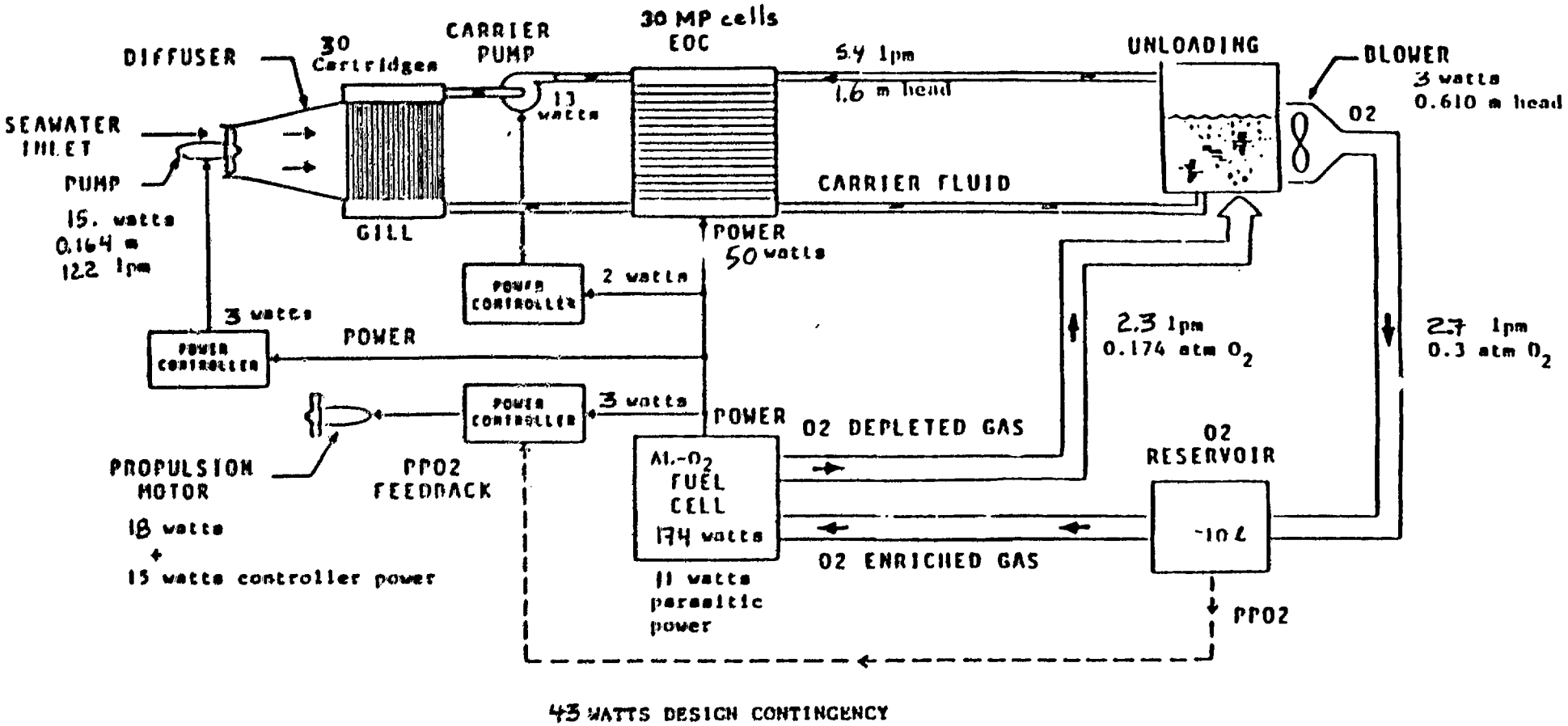

Fig. 15

4C. DARPA DEMONSTRATION VEHICLE DESIGN

Makai Ocean Engineering's (MOE) responsibilities during fiscal year 1988 were focused on the design, construction and testing of a seawater gill and seawater pump for the DARPA demonstration vehicle and the power unit demonstration. A brief summary and listing of major accomplishments over this period in each of these respective design categories follows:

Seawater Pump Design (See Figure 16)

Computer modeling of the demo vehicle power system indicated that the seawater pump would be the second largest energy consumer in the proposed vehicle next to the EOC unit itself. Therefore, it was important to identify a pump that could yield the required efficiency under the unique, extremely low head and low power conditions required by the vehicle system. An exhaustive search of the commercial pump market led to the conclusion that a custom design reciprocating piston pump had the best chance of filling the demo vehicle power system requirements. A list of activities carried out in pursuit of a high efficiency seawater pump are included below:

- Research and analysis of existing off-the-shelf pump candidates.
- Construction of a computer model of reciprocating piston pump and performance of sensitivity analysis of pump performance.
- Construction of 1/10th Scale Prototype Seawater Pump (custom piston pump) for testing and model verification
- Research and test small dc motors and gearboxes to couple with the piston pump head.
- Conceptual design of piston pump for demo vehicle.
- Detailed final design of 3-cylinder acrylic piston pump (see Figure 16).
- Specification and purchase of pump components and raw materials for fabrication.

The seawater pump development was halted just short of manufacture; some of the component parts were returned while others remain as inventory at MOE.

Seawater Gill Design (See Figures 17 and 18)

Previous preliminary design and modeling work indicated that a seawater gill unit could be most cost effectively designed based on the use of the CD Medical membrane cartridges. These CD modules were the building blocks from which a large surface area gill array could be assembled. To use these membrane modules, a number of tests were required to characterize their hydraulic performance and O_2 flux capabilities. Then a housing and filter system could be designed to accommodate them. MOE activities in FY 1988 as the lead design member for the seawater gill included the items listed below:

- Construction and testing of a 1/3 scale seawater gill module (12 cartridge radial design) to:
  1. Verify head versus flow relationships on the seawater circuit.
  2. Verify head versus flow relationships on the carrier circuit.
  3. Investigate flow equalization problems between cartridges on both the seawater and carrier circuits.

4. Design review and critical analysis of radial gill design.

- Redesign of gill cartridge unit into a smaller hull diameter using "3 across the beam" vertical orientation of the cartridges.
- Design and coordination of O_2 flux/permeability tests at Aquanautics.
- Redesign of cartridge end cap headers.
- Design of aluminum hulled gill unit to house up to 42 membrane cartridges, 30 filter cartridges, the seawater pump and to serve as major section of eventual demo-vehicle hull (see Figure 19).
- Specification and purchase of parts for gill unit.
- Leak testing and screening of cartridges for gill unit.
- Construction of mock-up gill unit for manifold testing.

The fabrication of the gill unit housing (see Figure 19) was halted after the fabricator had ordered aluminum stock and begun fabrication. The rolled aluminum hull sections, bulkheads and sheet stock remain as inventory at MOE.

SEAWATER PUMP
DETAIL DESIGN DRAWINGS

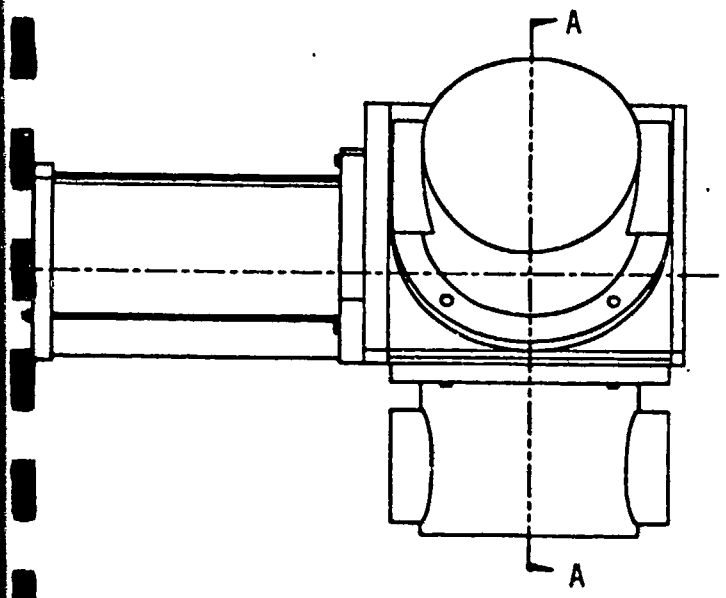

SIDE VIEW

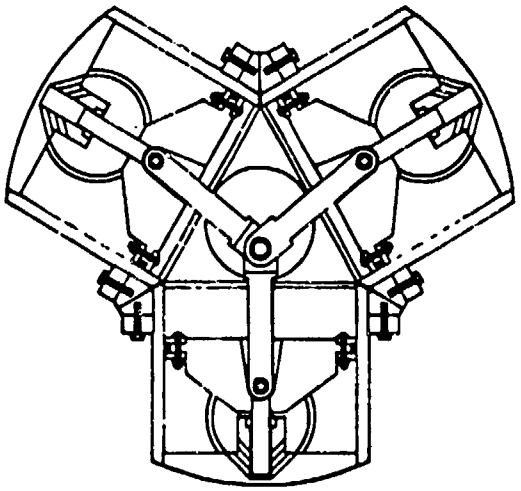

SECTION A-A

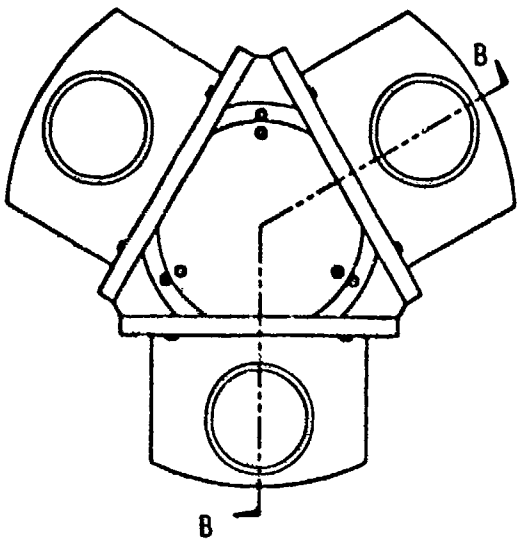

END VIEW

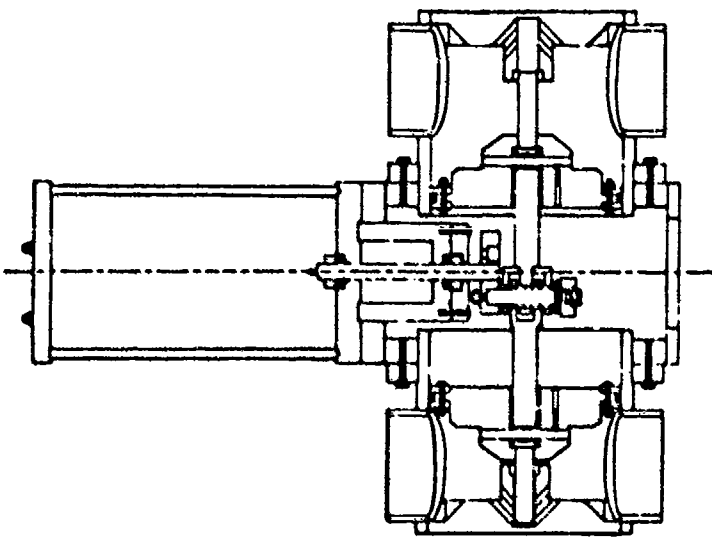

SECTION B-B

Fig. 16

MEMBRANE CARTRIDGE ARRANGEMENT
FOR DEMO VEHICLE GILL UNIT

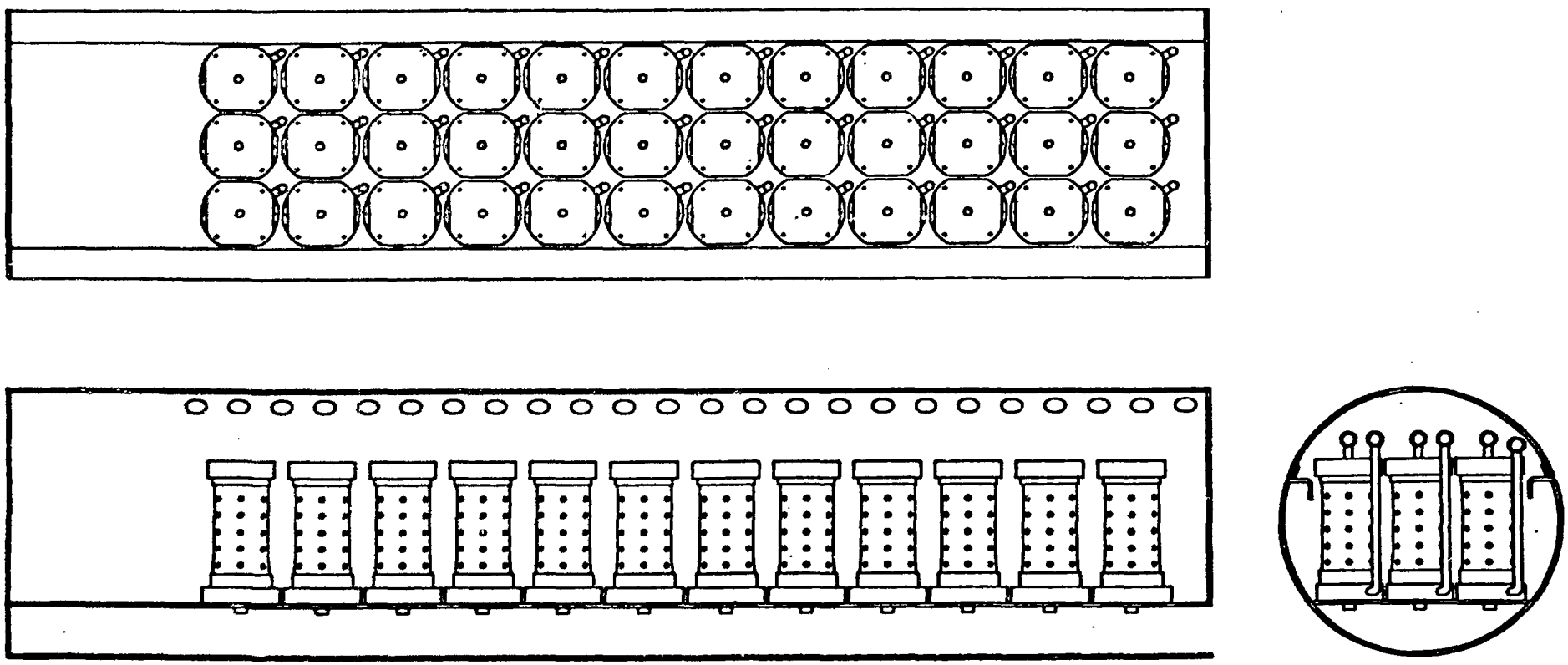

Fig. 17

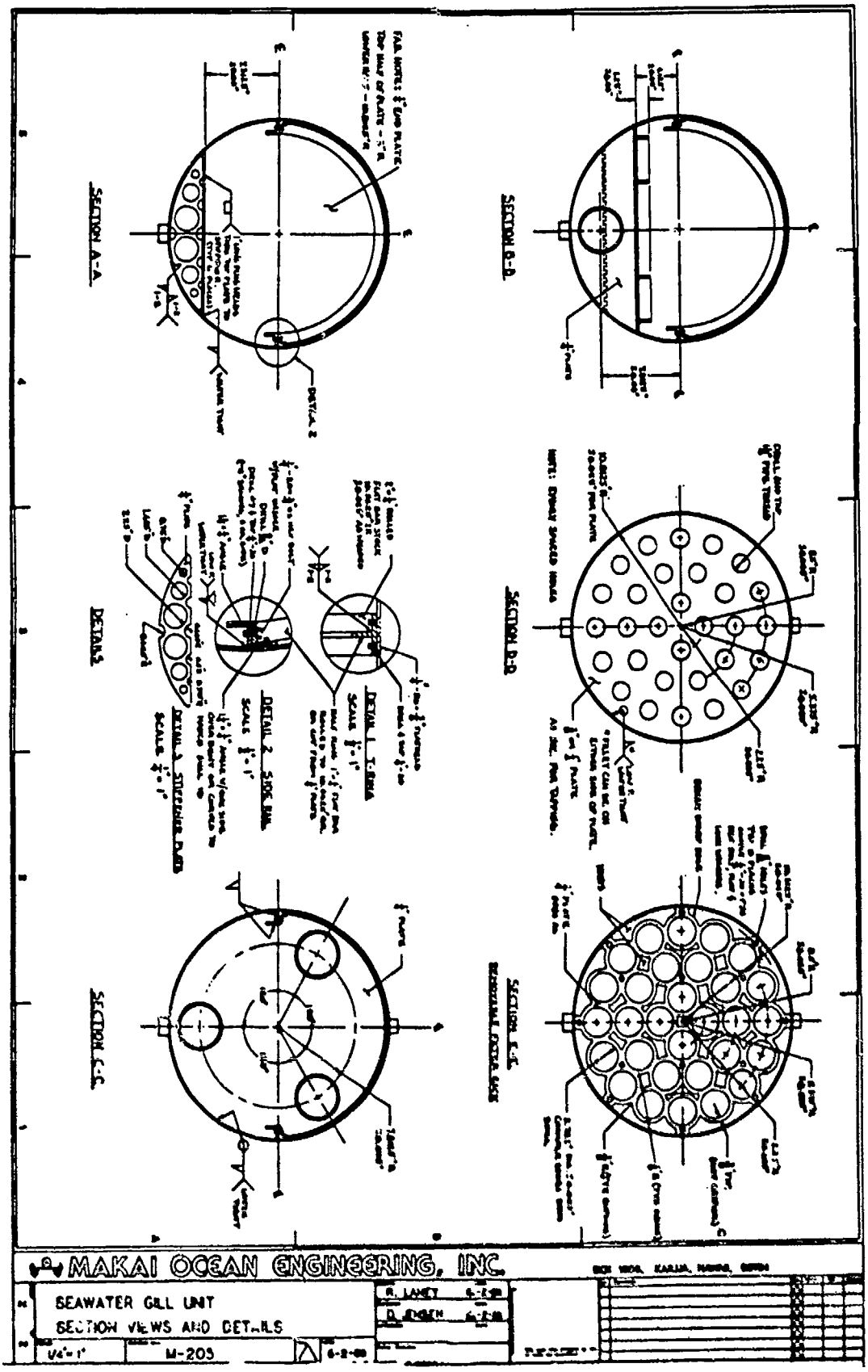

Fig. 18

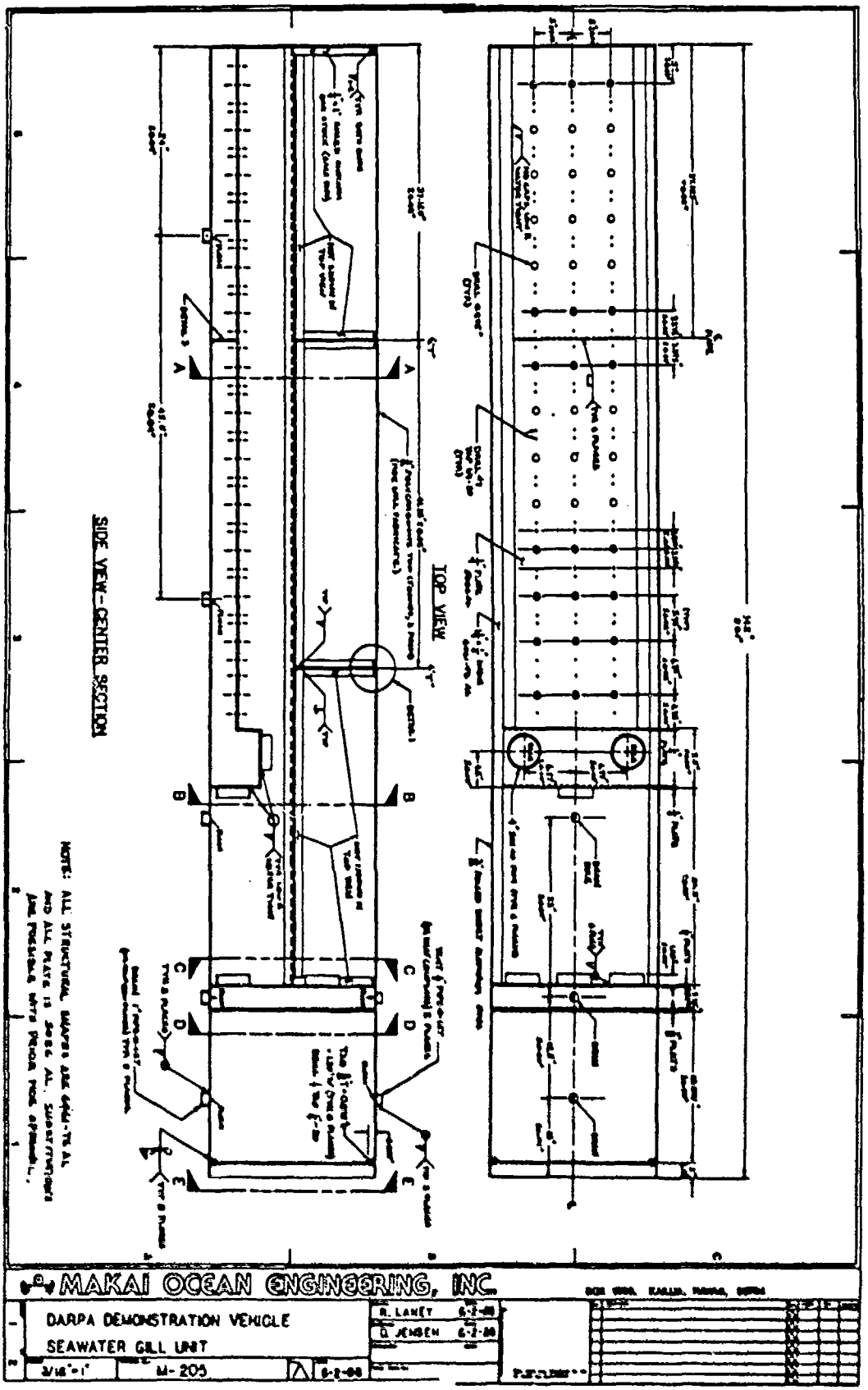

Fig. 19

4D. GILL: OXYGEN FLUX STUDY

Introduction

The gill portion of the Aquanautics AUV uses a series of micro-porous hollow fiber membranes. The free oxygen in the seawater defuses passively across the membrane into the carrier solution. The rate of oxygen flux across the membrane determines the size of the gill system. Oxygen flux can be maximized by optimizing the flow rates of carrier and seawater, such that oxygen flux is high and carrier and seawater pumping energy is minimal. Higher oxygen flux rates permit the use of smaller gills.

Carrier optimization which was carried out prior to O_2 flux study across gill produced a carrier with a very low vapor pressure. Seawater has a vapor pressure higher than carrier. Water vapor will travel across a concentration gradient from high to low vapor pressure. To prevent water flux through the membrane, in the form of water vapor, the vapor pressure of the two solutions must be matched. The matching of the vapor pressures of the carrier to the seawater required changing the carrier conditions.

Experimental

Hydrochloride crystals of the Compound #64 carrier, which had been optimized for oxygen output with air loading, were used as a baseline carrier. The carrier was later changed to Compound #64 freebase due to water vapor problems associated with vapor pressure differences across the membrane.

Carrier solution was circulated through the electrochemical cell into a split flow seawater and air loading system (see Figure 20). The split flow system allowed the carrier flow rate through the loading module to be changed, but ensured that the carrier which returned to the electrochemical cell was fully loaded with oxygen. The fully loaded carrier allowed the electrochemical cell to operate at a constant fractional conversion, thus avoiding any changes in carrier performance. This system was used to evaluate the flux of oxygen from seawater to carrier, and allowed for optimal performance.

Oxygen flux was determined by measuring the depletion of oxygen in the seawater feed. This is accomplished by measuring the the partial pressure of oxygen in seawater using YSI Clarke oxygen probes and calculating the oxygen solubility in seawater from values published in relevant literature. Seawater was run at 9-11 degrees Celsius. The seawater was made from Instant Ocean (Aquarium Systems, Mentor, OH) mixed to a concentration of 33 parts per thousand (ppt) using refractive index measurements. This concentration of 33 ppt matches that of the seawater 17 miles off the California coast at a latitude of 38°.

The gill membrane is a packaged 6 square meter module marketed by CD medical, Inc. The membrane module was chosen for its low pressure drop on the seawater side of the membrane. Carrier flow rates between .1 to .5 liters per minute and seawater flow rates between 3 to 8 liters per minute were used as experimental parameters.

Figure 20
Seawater-Carrier Oxygen Loading Test Layout

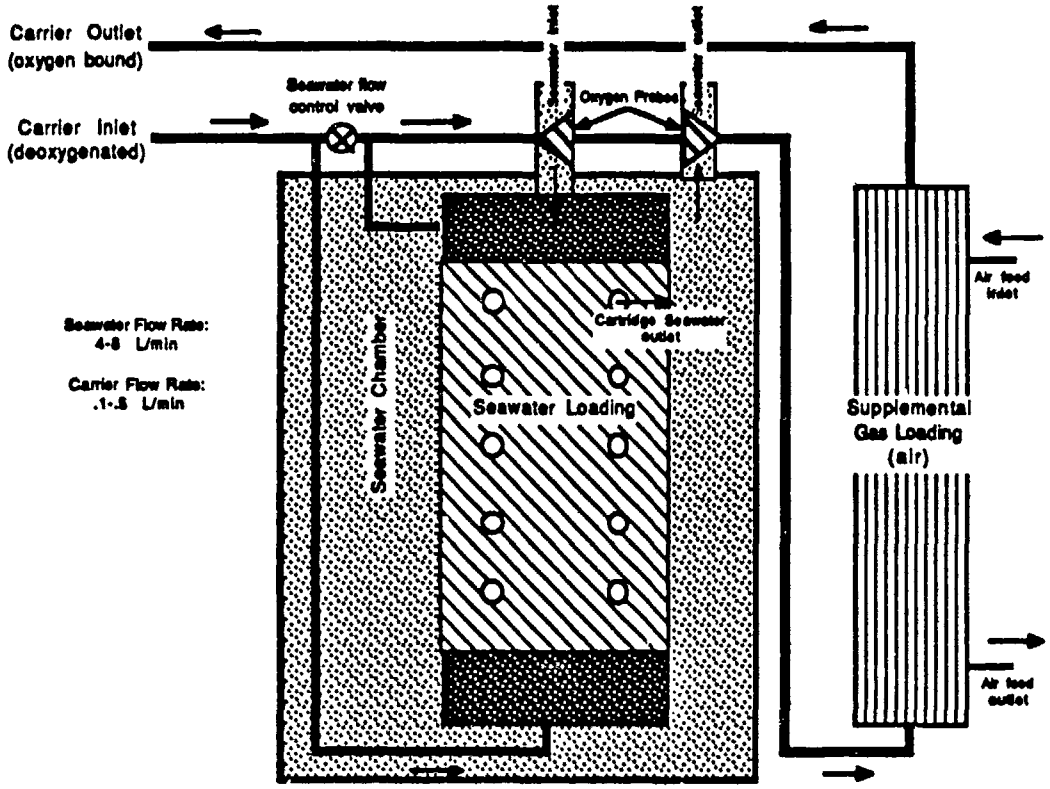

Results

Previous flux rate experiments were carried out with low concentrations of de-oxygenated carrier. These low concentrations of carrier (20 mM) were equivalent to the portion of de-oxy carrier found in a functioning carrier solution. Previous testing was run with 100 percent of the low concentration carrier being de-oxygenated. The carrier was not electrochemically recycled for oxygen re-binding.

The first flux experiments run with the up to date optimized carrier, revealed that a vapor pressure difference in the carrier caused water vapor to travel across the membrane. The rate of water vapor migration into the carrier was initially .027 liters of liquid water per hour per square meter of membrane. To keep water vapor from traveling across the membrane, the vapor pressure of the carrier was reduced to match the vapor pressure of the seawater. This was done by reducing the solute concentration of the carrier, using freebase Compound #64 (rather than the hydrochloride crystals), and eliminating the addition the electrolyte potassium chloride. For water loading, the optimal concentration was determined to be 430 mM Compound #64 (freebase) and 8 mM catalyst.

The collection of reliable flux data was hindered by a leaky batch of CD Medical cartridges. Changes have been made by CD Medical to correct the leaks. Aquanautics received and tested new modules incorporating these changes. The new cartridges performed without any leaks. Oxygen flux values were lower than in past experiments conducted with leaky cartridges exhibiting water vapor transfer.

Discussion

Prior to using carrier which had been optimized for high oxygen output, all flux experiments were run with carrier which had a vapor pressure close to the vapor pressure of seawater. In these experiments carrier was not recirculated through the system, but rather run through the loading module in one pass at a concentration equal to that of the portion of carrier which is available to bind carrier.

The optimization of carrier which was performed by using air as an oxygen source proved to be unsuited to underwater applications. The problem was an influx of water into the carrier in the form of water vapor. This was diluting the carrier and causing a decrease in performance proportional to the carrier dilution. Methods for extracting the water proved too costly in terms of energy required. With water removal being too costly and carrier dilution affecting performance, the only alternative was to sacrifice some performance of the electrochemical cell and run the carrier at a lower vapor pressure. The total size of the gill was not affected by the water vapor problem. Only the electrochemical cell performance and the volume of carrier associated with the cell were influenced.

Experiments carried out with the low vapor pressure carrier were focused more on checking the reliability of the corrected CD cartridges, than obtaining precise flux data. At the time that reliable membrane modules were acquired, the focus of the DARPA project was moved away from the AUV project towards a deep water power station.

Conclusion

Carrier conditions had to be changed from compound 64 hydrochloride crystals to compound 64 freebase. This decreased the conductivity of the carrier and decreased the cell performance from 2 liters per square meter to 0.6 liters per square meter of oxygen output.

This experimentation renewed confidence in the reliability of the CD Medical membrane modules. Further testing on oxygen permeability will require that published values for oxygen solubility used in oxygen flux calculations be cross checked to confirm their reliability. A second type of oxygen probe should also be employed in seawater oxygen partial pressure measurements as a cross check for the Clarke type probe.

As new carriers are developed, oxygen binding rates should be looked at as they affect the loading kinetics and gill size needed to produce excess power.

4E. EVALUATION OF THE ELTECH FUEL CELL

Introduction

Aquanautics received the final shipment of the Eltech fuel cells. Experiments were done to check the cell performance with respect to cell voltage, lifetime and shunt current losses. The minimum operating requirements set by Aquanautics were met.

Procedure

The fuel cell could be automatically operated. The system controllers could maintain the optimum conditions for running the fuel cell. The cell voltage, current, air back pressure, KOH back pressure, and pO_2 were monitored. The flow rates were checked manually. The operating conditions were:

KOH flow	1.5 lpm ± .5 lpm
KOH concentration	8.3 M
KOH pressure	14" ± 4" H_2O
KOH temperature	61 C ± 2° C
O_2 (either air or pure O_2 fed into a closed loop)	2.5 X stoic. req.
Gas pressure	2" to 4" greater than KOH pres.
BDW aluminum anodes	

Data

Two stacks of 9 cells were tested. Stack #1 was run for 10 hours, Stack #2 was run for 5 hours. A typical set of data for the cells operating under the given steady state conditions are presented below.

	Open Circuit		With Current Load	
	Stack#1	Stack#2	Stack #1	Stack #2
	O Amp	O Amp	11.5 amp	11.0 amp
Individual Voltages	1.805	1.880	1.61	1.66
	1.746	1.818	1.63	1.57
	1.721	1.788	1.66	1.58
	1.689	1.803	1.57	1.58
	1.698	1.744	1.50	1.33*
	1.708	1.810	1.50	1.61
	1.657	1.772	1.33*	1.48
	1.725	1.806	1.58	1.56
	1.759	1.826	1.60	1.59
Measured Total	15.48	16.30	13.30	13.70

*The cathodes in these cells may be defective. They will be replaced.

Results & Discussion

All of the cells have been tested. Potentially defective cathodes have been returned for replacement. Shunt current losses in the cell do not need to be dealt with at this time.

When cell #1 was run, a green substance was found to have coated the cathodes. A few of these cells were included in run #2. The mysterious coating did not seem to affect their performance.

The BDW anodes vary widely in quality. The anodes in cell #2 were more thoroughly cleaned than in cell #1 and the edges of the anodes were checked

for flatness to ensure a proper gasket seal. The slightly better performance of cell #2 is probably due to the better anode preparation.

The final electrolyte system for the DARPA demonstration has been received.

4F. FUEL CELL-EOC INTEGRATION

A small-scale integration of the fuel cell and electrochemical cell was carried out to check the compatibility of the two systems. The carrier from the anode of the electrochemical cell containing oxygen in a two-phase mixture was pumped to an unloader. The unloader was essentially a sparge tower, where the carrier-oxygen mixture was poured down into a pool at the bottom of the column. Oxygen depleted gas from the fuel cell was used to sparge the carrier and remove the gaseous oxygen mixed with it. The oxygen rich product of this operation was then fed to the fuel cell for consumption. Figure 21 depicts a schematic of this integration. The following parameters were monitored during the experiment:

1. Voltage of EOC and fuel cell
2. Current of EOC and fuel cell
3. pO_2 in gas circuit (Item 12 in Figure 21)

The pO_2 change in the gas loop determines whether the fuel cell is consuming the same amount of O_2 as the amount that the EOC is generating. If the pO_2 is steady, then the O_2 generated from the EOC is the same as that consumed by the fuel cell.

These trial runs were completely satisfactory. The power produced by the fuel cell was commensurate with the oxygen produced and the design point was fully verified.

Details of the runs are given in Figures 22 and 23. The integration met or exceeded the design specifications of the demonstration vehicle, the fuel cell provided power at 410 W-min/l of O_2 consumed. The EOC provided O_2 at a power cost of 102 W-min/l of O_2 produced.

FUEL CELL SYSTEM DIAGRAM

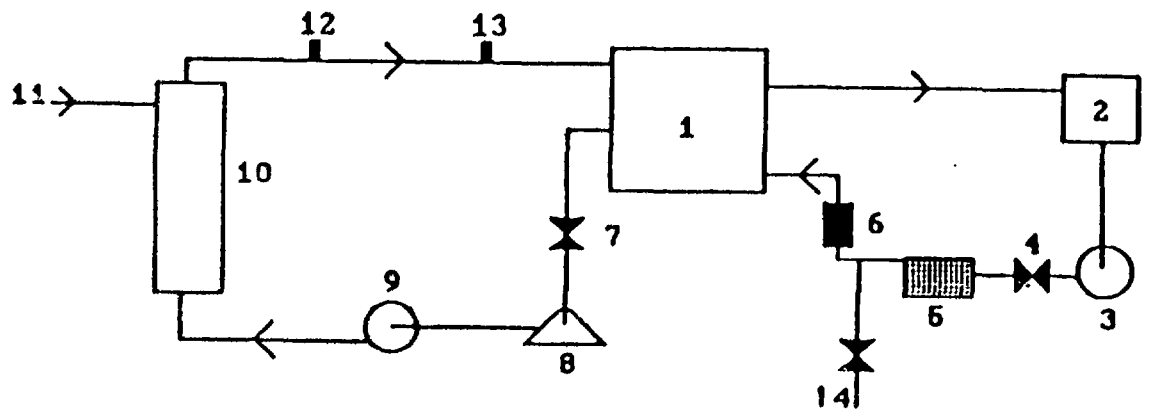

1. *Eltech Cell*
2. KOH Holding Tank
3. Caustic Pump
4. Flow Control Valve
5. Heat Exchanger
6. Flow Meter for Caustic
7. Gas Backpressure Valve
8. Condensate Trap
9. Gas Loop Pump
10. Gas Mixing Chamber or E.O.C. O_2 Unloader
11. Pure O_2 or E.O.C. Oxygen
12. pO_2 Monitor
13. Cathode Backpressure Monitor
14. Drain Valve

Fig. 21

RESULTS OF INTEGRATION

P_{O_2} = 0.32 ATM

FUEL CELL	EOC
V = 1.5	V = 0.5
A = 12 - 12.5	A = 9
Watts = 18 - 18.25	W = 4.5

Theoretical ratio of $\frac{\text{Fuel Cell Power}}{\text{EOC Power}} = \frac{410}{102} \cong 4$

Actual = 4.0 - 4.2

Fig. 22

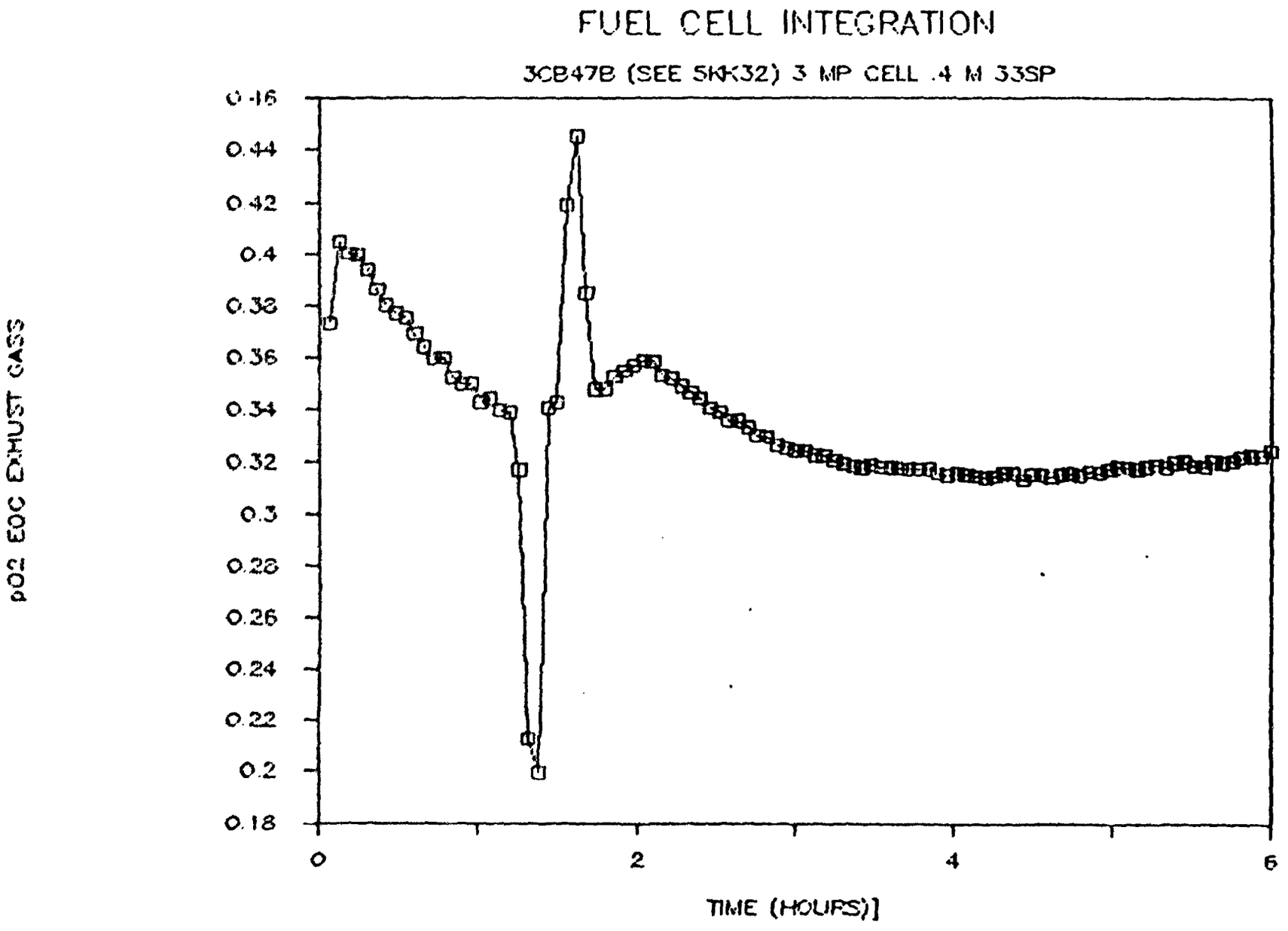
FUEL CELL INTEGRATION
3CB47B (SEE SNK32) 3 MP CELL .4 M 33SP
pO2 EOC EXHUST GASS
0.46
0.44
0.42
0.4
0.38
0.36
0.34
0.32
0.3
0.28
0.26
0.24
0.22
0.2
0.18
0
2
4
6
TIME (HOURS)]

Fig. 23

4G. CONCLUSION

The AUV demonstration program was on schedule as was originally planned. Hardware that was purchased or fabricated is listed below:

1. Cells
2. Fuel Cell
3. Gill Cartridges
4. Portion of the Hull

Design was completed for the whole system.

Oxygen flux study and some scale-up issues were being worked on when this AUV demonstration project was put on hold.

5. ENGINEERING TOWARDS UNDERWATER STATIONARY POWER SYSTEM

In July 1988, work towards the development and design of the underwater stationary power system began. This section summarizes the progress up to date.

The heart of an underwater stationary power system will be either a battery or a fuel cell. This depends on the power delivered and endurance. A fuel cell will normally be more applicable at higher powers and greater endurance. Figure 24 shows relative application areas of fuel cell and batteries. The fuel cell technology has developed such that fuel cells themselves are fairly compact and light. For example, a 15 kW fuel cell takes about 5 ft^3 of space but the reactants (H_2 and O_2 stored at 6000 psi) would need a volume of 78 ft^3 for an endurance of 82 hours of operation[5]. Stored gas at 6000 psi is not easily available and gas at 3000 psi will need even larger volumes. For the same operation an Ag-Zn battery system, with highest power density among all proven rechargeable systems, would need a volume of 420 ft^3 with an equivalent price tag. Moreover, this data is for an endurance of less than 4 1/2 days only. It is therefore clear that reactants take up most of the volume and weight for long endurance power systems.

5A. CONCEPT DEVELOPMENT

For a long endurance power system, a fuel cell with reactants produced in-situ would be ideal, provided that the systems to produce the reactants displace less volume when compared to stored reactants. Aquanautics is investigating the feasibility of such a system. In this scheme, oxygen is generated by Aquanautics gill system and H_2 is generated by an Al-H_2O system.

Oxygen Generation

The main assumptions underlying development of this power system concept are:

1. A pressure vessel to house the power system at 1 bar will be too expensive and is not considered. The system therefore is to operate at ambient pressure.

2. The Aquanautics carrier cannot operate at high pH.

3. Oxygen produced at the electrochemical cell will remain dissolved in the carrier at the pressures involved.

[5]D. McVay, International Fuel Cells; Presentation at MIT Sea Grant Symposium, October, 1988.

ENERGY MAP

O_2 EXTRACTION POWER VS NUCLEAR AND BATTERIES

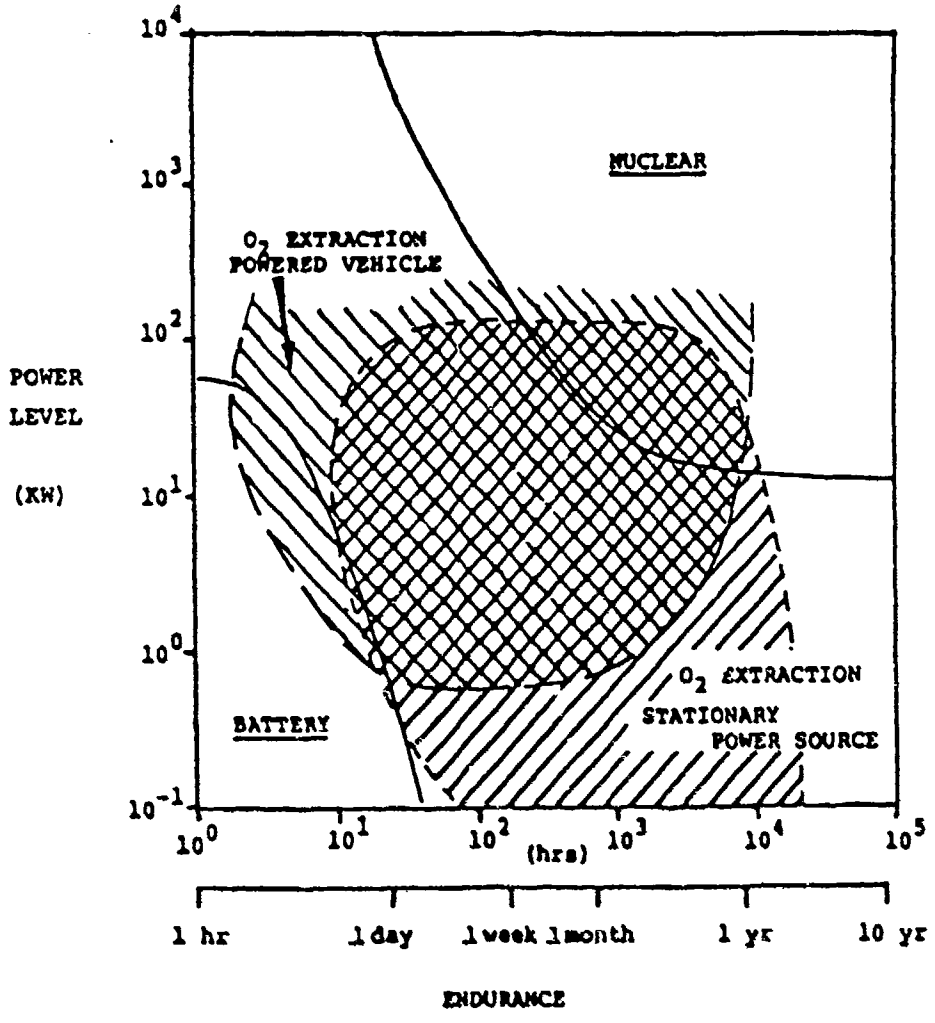

Fig. 24

With the above assumptions, the following becomes obvious:

- Case 1. Carrier has to deliver the oxygen in the fuel cell itself; or
- Case 2. O_2 transfer from the carrier to the electrolyte in the fuel cell has to take place through a solid membrane.

Case 1: Here the carrier comes directly in contact with the fuel cell electrode and other materials. This requires a new fuel cell design with the following advantage and disadvantage.

Advantage: No three-phase design is necessary as the oxygen is dissolved in a liquid, namely the carrier.

Disadvantage: Material selection (electrode, membrane, etc.) becomes more critical

Oxygen reduction in a fuel cell increases pH. There will be a microscopic pH gradient from the electrode surface to the bulk electrolyte and a macroscopic gradient from the membrane surface to the interior of the fuel cell bed. The pH change may also affect the properties of the carrier.

Since the carrier cannot operate at high pH, an overall acid or base neutrality must be maintained. This implies that an H_2 - SPE fuel cell concept should be employed. The H_2 will provide the necessary H^+ ions to counteract the OH^- build up at the other electrode.

Case 1 can further be divided into two sub-cases:

- Case 1A. This is the simplest case (Figure 25). Here carrier picks up O_2 through a solid membrane from seawater and delivers it at the fuel cell. There is no electrochemical cell. The carrier itself acts as a concentrator of O_2 in a bound form, such that large quantities of seawater do not have to be flown through the fuel cell. Instead, a smaller flow rate of carrier needs to be flown through the fuel cell. In the fuel cell, cathode consumes O_2. Seawater at these depths carries about 3 ml of oxygen/l whereas carrier can bind up to 4 l of oxygen/l. Nevertheless, large quantities of seawater have to be passed through the system, but a specially designed gill system may handle that better than an intricate design such as a fuel cell. One of the operational characteristics of this system would be low oxygen partial pressure (pO_2) everywhere. Computer modeling will be carried out to determine whether this will have any detrimental effect on the efficiency of the system
- Case 1B. This is similar to the previous system except that an electrochemical cell is superimposed between gill and the fuel cell (Figure 26). The function of the electrochemical cell is to boost the pO_2 in the carrier

that enters the fuel cell. This scheme will be explored in the event that Case 1A is not viable.

Case 2: See Figure 27. In this case, carrier delivers O_2 to the electrolyte in the fuel cell through another membrane. Here an electrochemical cell is mandatory. The difference in pO_2 across a membrane is the driving force for oxygen transfer. If the pO_2 difference is small (less than 0.2 atmosphere), the area of membrane surface in the fuel cell will be large and of the same order of magnitude as the gill area. However, an electrochemical cell will alleviate this problem, the pO_2 in the carrier can be raised and this will lead to much lower membrane area. One advantage of this scheme is that the carrier does not come in contact with fuel cell electrode. Therefore the choice of fuel cells can be broadened significantly.

Figure 25

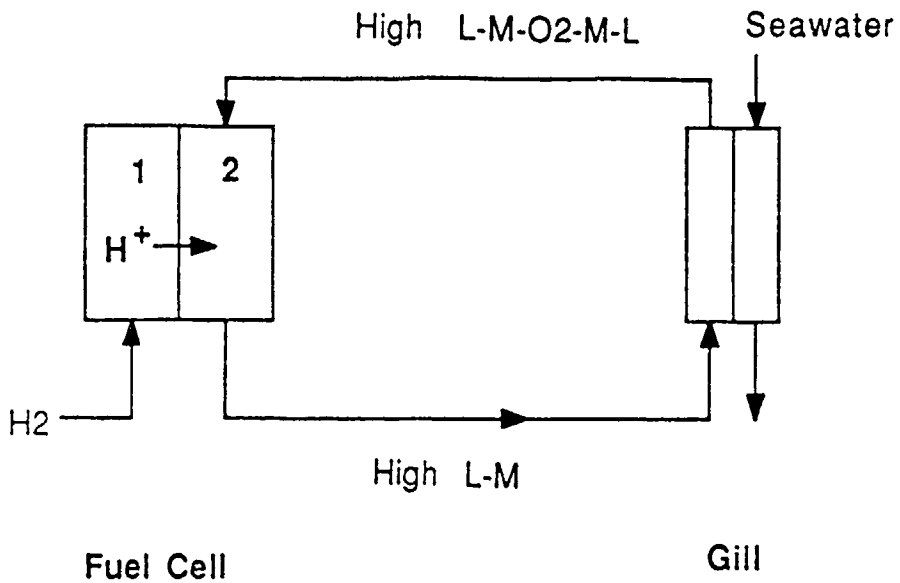

Reactions:

Fuel Cell

at 1. $2H_2 \rightarrow 4H^+ + 4e^-$

at 2. $[O_2]_d + 2H_2O + 4e^- \rightarrow 4OH^-$ at electrode

$L\text{-}Co^{II}\text{-}O_2\text{-}L \rightarrow 2LCo^{II} + [O_2]_d$ in the bulk

Gill

$2L\text{-}Co^{II} + [O_2] \rightarrow L\text{-}Co^{II}\text{-}O_2\text{-}Co^{II}\text{-}L$

Figure 26

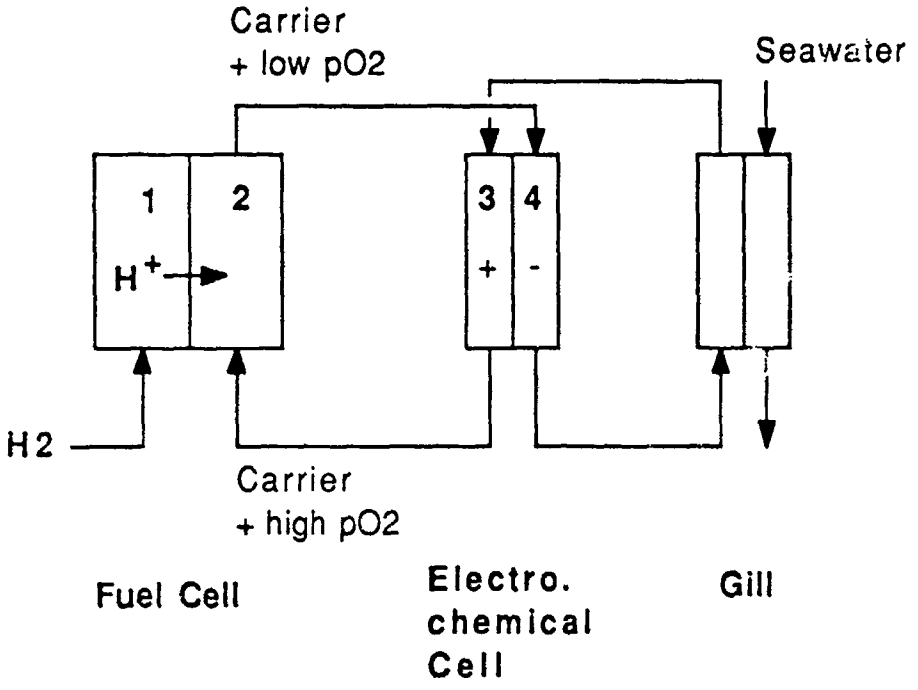

Reactions:

Fuel Cell

at 1. $2H_2 \rightarrow 4H^+ + 4e^-$ @ anode

2. $[O_2]_d + 2H_2O + 4e^- \rightarrow 4OH^-$ @ cathode

$2H_2 + [O_2]_d \rightarrow 2H_2O$ overall cell reaction

Electrochemical Cell

at 3. $L\text{-}Co^{II}\text{-}O_2\text{-}Co^{II}\text{-}L \rightarrow 2L\text{-}Co^{III} + [O_2]_d + 2e^-$

at 4. $2L\text{-}Co^{III} + 2e^- \rightarrow 2L\text{-}Co^{II}$

$L\text{-}Co^{II}\text{-}O_2\text{-}Co^{II}\text{-}L \rightarrow 2L\text{-}Co^{II} + [O_2]_d$ overall cell reaction

and at gill

$2L\text{-}Co^{II} + O_2 \rightarrow L\text{-}Co^{II}\text{-}O_2\text{-}Co^{II}\text{-}L$

Figure 27

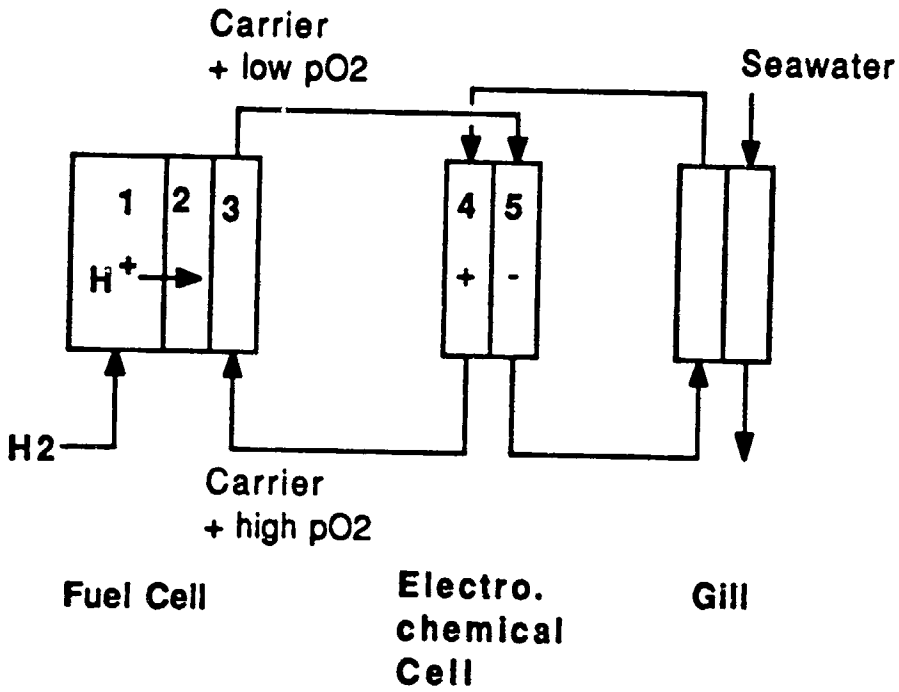

Reactions:

Fuel Cell

at 1. $2H_2 \rightarrow 4H^+ + 4e^-$

at 2. $[O_2]_d + 2H_2O + 4e \rightarrow 4OH^-$

at 3. No reaction.

Electrochemical Cell

4. $L\text{-}Co^{II}\text{-}O_2\text{-}Co^{II}\text{-}L \rightarrow 2L\text{-}Co^{III} + [O_2]_d + 2e^-$

5. $$\frac{2L\text{-}Co^{III} + 2e^- \rightarrow 2L\text{-}Co^{II}}{L\text{-}Co^{II}\text{-}O_2\text{-}Co^{II}\text{-}L \rightarrow 2L\text{-}Co^{II} + [O_2]_d}$$

Gill

$$2L\text{-}Co^{II} + O_2 \rightarrow L\text{-}Co^{II}\text{-}O_2\text{-}Co^{II}\text{-}L$$

Hydrogen Generation: In-situ hydrogen generation can be carried out in the following ways:

1. Steam reforming of methanol
2. Use of LiH_2, Borohydride
3. Al-H_2O reaction, Li-H_2O reaction

Off-course, cryogenic or high pressure H_2 are the conventional ways to carry the fuel. Other liquid fuel, e. g. hydrazine, for fuel cells had been tried. These methods are either abandoned or in early stage of development.

Figures 28, 29 and 30 compare steam reforming of methanol and Al-H_2O reaction with cryogenic hydrogen. Use of LiH_2, borohydride, Li-H_2O is not considered as they are known to lead to unstable and/or unsafe and/or prohibitively expensive systems.

Al-H_2O scheme chosen is as that of Al-Watt system marketed by Alupower Inc., as a battery. This also produces reasonable amount of energy accompanied by H_2 generation. Overall cell reaction is

$$Al + 3H_2O \text{ ---> } Al(OH)_3 + 3/2\ H_2\uparrow$$

Aquanautics is considering Al-H_2O system as H_2 producer. The extra amount of energy will also be useful. The main features of the Al-watt system[6] are:

w-Hr/kg	w-Hr/liter	H_2 production at STP	
		l/l of system	l/kg of system
455	900	1400	708

It is to be noted that an H_2 O_2 fuel cell system produces approximately 100 w-min/l or 1.67 w-hr/liter of H_2.

In the next section, this scheme of H_2-generation will be included in the comparative analysis.

[6]Alupower Inc., Brochure, Alwatt System.

MAKAI OCEAN ENGINEERING, INC.
14-Oct-88

NET SYSTEM ENERGY DENSITY COMPARISON

	PLOT 1						PLOT 2				PLOT 3
MASS BASIS	"E"	"K"		"N"	"G"	N(1-GK)	"EX"	E(N(1-GK))+EX		"F"	F(E(N(1-G
FUEL SYSTEM	FUEL SYST ENERGY DENSITY	O2 REQM'T	CONVERTER SYSTEM	CONV. EFF.	O2 PWR REQM'T	NET CONV EFF.	EXTRA NON-O2 CONSUMING E. DENSITY	NET SYST ENERGY DENSITY	FUEL SYSTEM DENSITY	NEUTRAL PACKING FACTOR	NEUTRAL NET ENERG DENSITY
	WH/KG	LPS O2/ /WATT			WATT/ /LPS O2		WH/KG	WH/KG	KG/M3		WH/KG
METHANOL	5192.1	8.65E-05	ACID FC	58.0%	2818.6	43.9%	0	2277.2	813	0.7772	1769.8
H2-CRYOGENIC	6230.5	7.26E-05	SPC FC	58.4%	2831.1	46.4%	0	2890.7	380	0.3489	1008.6
ALWATT-H2	6510.6	7.26E-05	SPE FC	58.4%	2806.5	46.5%	455	1622.5	2660 *	0.7564	1227.2
VOLUME BASIS	WH/L						WH/L	WH/L			WH/L
METHANOL	3837.3	8.65E-05	ACID FC	58.0%	2818.6	43.9%	0	1683.0	813	0.9799	1649.1
H2-CRYOGENIC	1838.2	7.26E-05	SPC FC	58.4%	2831.1	46.4%	0	852.9	380	0.9411	802.7
ALWATT-H2	5046.7	7.26E-05	SPE FC	58.4%	2806.5	46.5%	900	3618.8	2660 *	0.2915	1054.8

* ASSUMED BASED ON ESTIMATED DISPLACEMENT VOLUME, ALUPOWER DATA DOES NOT STATE IF THEIR VOLUMETRIC DATA IS FOR DISPLACED VOLUME OR OCCUPIED VOLUME.

Fig. 28

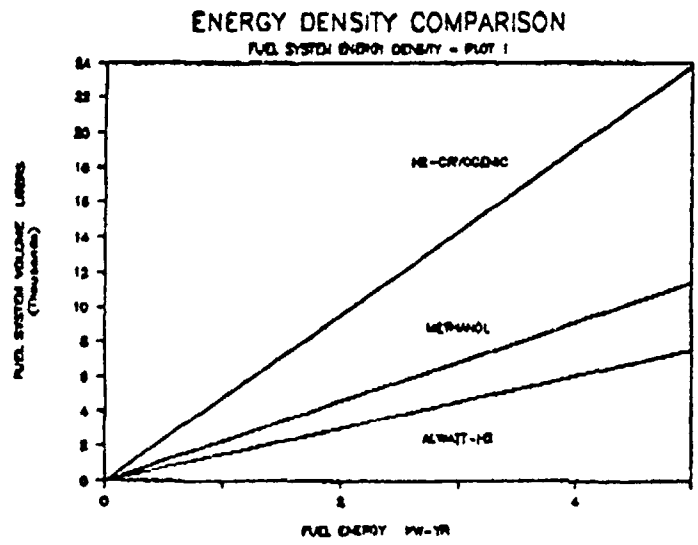
ENERGY DENSITY COMPARISON
METHANOL

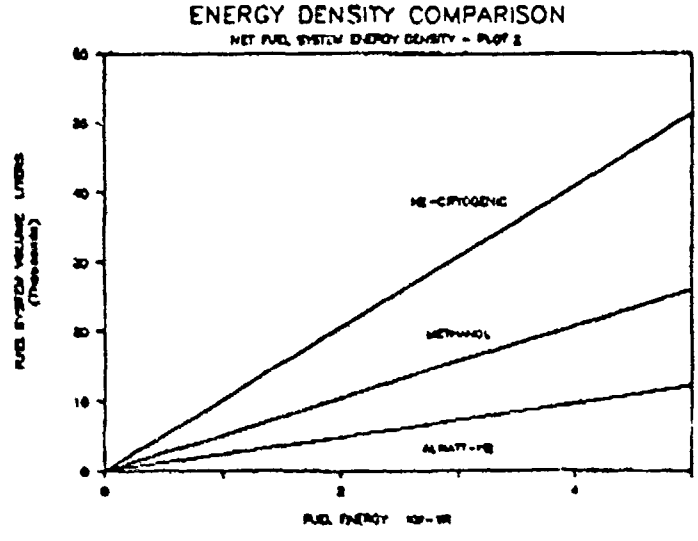
ENERGY DENSITY COMPARISON
METHANOL

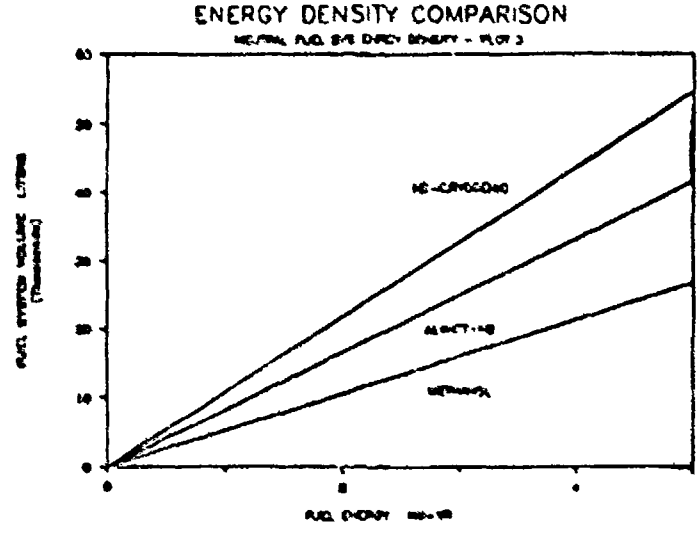
ENERGY DENSITY COMPARISON

Fig. 29

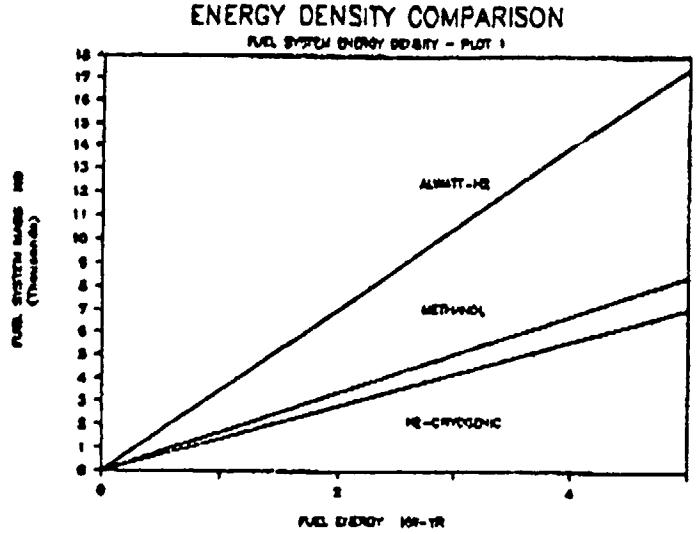
ENERGY DENSITY COMPARISON
METHANOL
0
2
4

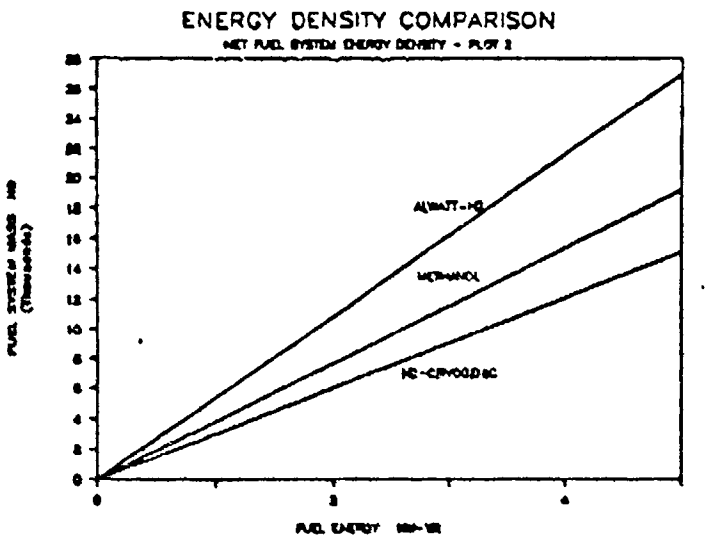
ENERGY DENSITY COMPARISON
METHANOL
0
3
4

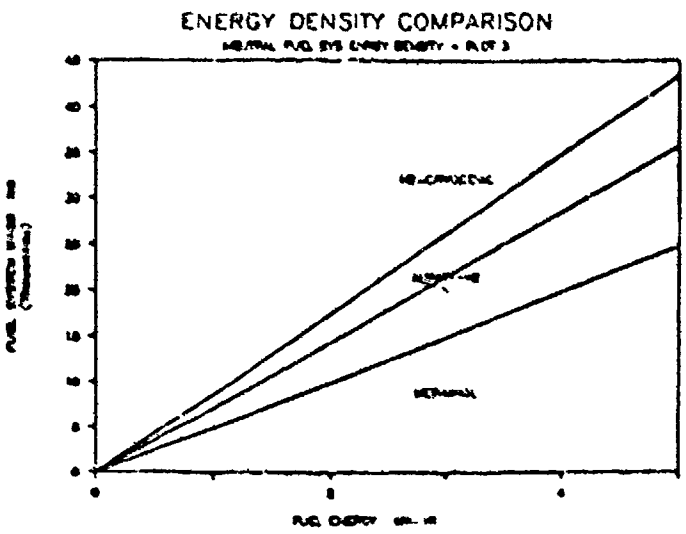
ENERGY DENSITY COMPARISON
0
4

Fig. 30

5B. ENERGY SYSTEM ANALYSIS

An Aquanautics' goal in the development of its electrochemical oxygen cell (EOC) for the Navy has always been to illustrate how this technology coupled with an appropriate high energy-density and high O_2-efficiency energy converter can form a complete high energy density power system. Such a power system may have many Navy applications if it provides superior performance over competing power system technologies.

In order to compare the EOC/O_2 extraction system technology coupled with various energy converters to the competition, Aquanautics has developed with the assistance of Makai Ocean Engineering, Inc. several computer models that incorporate these different power system technologies into stationary sea floor power plants, underwater systems including long range AUV's, sprint and drift AUV's and even large submarine tanker vessels. This section first identifies the various power options for a stationary power source and then shows the comparison in such a system as calculated by the computer model. The following description does not include any other systems analysis such as AUVs because they have been demonstrated extensively in previous program documents.

Alternative Energy Systems

At the outset it is necessary to identify the competition to the EOC/energy converter power system and point out the important characteristics, advantages and disadvantages of each. The list below presents all of the power system options Aquanautics has identified as possible competition to the EOC/energy converter power system:

Stored O_2 technologies (which could be coupled with high energy density energy converters and fuel systems):

1. O_2 stored in steel storage vessels at 3000 psi
2. O_2 stored in filament wound fiber vessels at 3000 psi
3. O2 stored as a liquid in cryogenic dewars

Battery Technologies:

1. Lead-Acid deep cycle rechargeable storage batteries
2. Silver-Zinc rechargeable storage batteries
3. Lithium/Thionyl Chloride primary batteries
4. Magnesium-O_2 seawater batteries

A brief discussion of each of these alternatives is presented in the following paragraphs.

Stored O_2 Systems - Steel Storage Vessels: High pressure steel storage tanks are the current industry standard for storage and transport of O_2 and other industrial gases. Therefore, they are a readily available means of providing O_2 to an energy converter in the underwater environment. Their principal drawback is their weight per unit O_2 stored. Steel bottles holding 3000 psi O_2 provide a system weight 7 times greater than the weight of the O_2 being stored. This number could be lowered through the optimization of the

pressure, size, shape and materials of the storage vessels, but there will always be a large weight penalty associated with steel O_2 bottles. In submerged applications which require power systems of neutral buoyancy, steel storage bottles require the addition of buoyancy such as syntactic foam, further adding to their weight and volume.

Stored O_2 Systems - Filament Wound Fiber (FWF) Storage Vessels: Filament wound fiber storage vessels are manufactured by Brunswick Corporation and have found wide use in the NASA Space Shuttle. Their major advantage to NASA is their light weight per unit O_2 stored. They are also capable of being pressurized to very high pressure up to as high as 20,000 psi, thus storing O_2 at densities rivaling liquid O_2. For marine applications their light weight is not necessarily an advantage, as large amounts of lead are required to submerge these vessels. Their cost, availability, ruggedness, and tolerance to seawater have never been thoroughly investigated. Aquanautics has restricted comparison to 3000 psi FWF bottles simply because the equipment to pressurize such vessels to higher pressures is not available on Navy vessels.

Stored O_2 Systems - Cryogenic Storage Vessels: Liquification of O_2 allows storage of the gas at its maximum density. This lowers system weight to approximately 1.3 times the weight of the stored O_2. The major drawback to cryogenic O_2 storage is the system complexity and fragility. Very low temperatures embrittle steel and other metals making maintenance and inspection critical to continued successful operation especially for shipboard applications where rugged conditions prevail. Cryogenic dewars are not perfect insulators, so there must be a continual bleed of O_2 from the storage vessels. For long endurance applications where large volume of liquid O_2 are required, this bleed could seriously drain the system's O_2 reserves prior to use and lead to an identifiable signature in covert missions. The high cost and poor availability of cryogenic O_2 and the plants and equipment to produce it are important drawbacks to its use. Conversations with Navy Personnel have shown that cryogenic gas storage is not a desirable option. Aquanautics does not examine cryogenic O_2 storage as an alternative in this study.

Batteries - Lead Acid: Lead acid batteries have been the standard submersible energy storage medium almost since the conception of submersible vehicles and power systems. Their advantages are many and are well known; they are low in cost, readily available, highly reliable, rechargeable, have good high rate discharge performance, high cell voltage, good low and high temperature performance, are rugged and easily pressure compensated. Their drawbacks are equally well known; they have very low energy density (<40 watt-hr/kg), poor charge retention, H_2 evolution during recharge, and permanent polarization of electrodes if stored in discharged condition. In these comparisons Aquanautics only considers the more advanced battery systems now under consideration by the Navy.

Batteries - Silver-Zinc: Silver-Zinc batteries have the highest energy density of any secondary battery, up to 100 watt-hr/kg or 200 watt-hr/l basis of any secondary battery. This has led to their growing use in submersible applications. They also list among their advantages good high rate discharge performance, a flat discharge voltage characteristic and low self-discharge. Major drawbacks to their use is their high cost, low cycle life, decreased

performance at low temperatures and sensitivity to overcharging. Although their energy density is the highest among secondary batteries, it is only a fraction of that obtainable with advanced primary cells discussed below. Aquanautics does not examine silver-zinc cells in the current comparisons.

Batteries - Lithium/Thionyl Chloride: The lithium/thionyl chloride primary cells have one of the highest energy densities of practical battery systems with energy densities ranging to 500 watt-hr/kg and 900 watt-hr/l. Their other advantages include high cell voltages to 3.9 V, relative insensitivity to temperature fluctuations, flat voltage discharge characteristics, and long shelf life. A principal disadvantage associated with lithium based cells has always been safety and the chance of explosion. This was primarily a problem with high discharge rate cells, which are not necessarily the type used in undersea applications, especially for long endurance applications. Relevant disadvantages include cost, availability and possibly transport restrictions. The lithium/thionyl chloride battery represents about the best practical competitor the battery industry can provide for comparison to the oxygen extraction/energy converter power system proposed by Aquanautics.

Batteries - Magnesium/O_2 Seawater Battery: Aquanautics information about this battery system has primarily originated from interviews and discussions with Ken Rogers at the Naval Ocean Systems Center (NOSC) in San Diego. Reports authored by NOSC about this seawater battery have claimed high energy density (to 440 watt-hr/kg), pressure compensated operation, low cost, mechanical rechargeability and indefinite shelf life among its advantages. However, like the Aquanautics' EOC this seawater battery is still under development. The best operational experience to date is a 10 kwh system with 1-2 watt output power at very low voltages. A configuration to deliver larger power outputs and higher voltages is still developmental. The battery is bulky and although its displaced volume will probably be reasonably small, it occupies a lot of space on board the submerged platform. Like the EOC system the seawater battery derives its oxygen from the seawater, thus large surface areas must be exposed to the passing water. This can lead to packing and configuration design difficulties especially for cell stacking to raise voltages. Also like the EOC gill system, the battery is susceptible to changes in the O_2 concentration of the seawater. Its principal advantage over the EOC/gill/energy converter system is that it concentrates its O_2 extraction,O_2 use and power delivery in one piece of hardware, thus reducing system complexity and hopefully providing improved reliability.

Systems Analysis

For this proposal, the computer model has been updated and tailored for analysis of stationary power systems. Many of the input parameters have been revised to reflect the wealth of new information we have available to us since the original vehicle model was constructed in 1985. The new stationary power system model has been used to carry out the following analysis:

1. A comparison of several possible energy converters for a stationary power plant using the EOC/gill technology.

2. A comparison of the gill/EOC technology coupled with fuel cells vs. competing power systems for stationary applications.

3. A parametric evaluation of the importance of the gill/EOC assumptions to the overall result.

Figure 31 is a tabulation of the important values assumed for various parameters relative to the stationary power system operating environment, the EOC/carrier system design, the gill design, and miscellaneous subsystem designs. These baseline values will be maintained for all comparisons conducted using the stationary power system model except as noted.

BASELINE VALUES FOR STATIONARY POWER SYSTEM

Environment:	
O2 CONCENTRATION IN SEAWATER	0.006 L/L
TEMPERATURE OF SEAWATER	10 DEG C
O2 SOLUBILITY IN SEAWATER AT THIS TEMPERATURE	0.0381 L/L/ATM
AMBIENT PRESSURE (ABSOLUTE)	11 ATM
FREE STREAM VELOCITY AT GILL	0 M/SEC
EOC/Carrier design:	
EOC UNIT POWER	25 WATTS/LPM
CARRIER OXYGEN LOADING	1.0 L O2/L CARRIER
CARRIER CONCENTRATION	0.4 MOLAR
DENSITY OF CARRIER SOLUTION	1140 KG/M^3
MOLECULAR VISCOSITY OF CARRIER SOLUTION	0.00141 KG/(SEC.M)
O2 SOLUBILITY IN CARRIER SOLUTION	0.0277 L/L/ATM
Gill Design:	
DIAMETER OF GILL TUBES, outside	0.23 MM
DIAMETER OF GILL TUBES, inside	0.2 MM
SEPARATION BETWEEN TUBE CENTERLINES	0.575 MM
TUBE ANGLE TO SEAWATER FLOW	25 DEG
EQUIVALENT GILL PERMEABILITY	0.0011 L/S/M^2/ATM
Miscellaneous Subsystem Design:	
CARRIER PUMP EFFICIENCY	50 %
WASTEWATER PUMP EFFICIENCY	50 %
PROPELLER EFFICIENCY (Seawater Pump)	65 %
GEARBOX EFFICIENCY (Seawater Pump)	85 %
MOTOR EFFICIENCY (Seawater Pump)	63 %

Figure 31

Figure 32 is a typical output tabulation illustrating one particular stationary power system design that has been optimized to achieve minimum weight and volume. It is useful to go over this figure to point out the important characteristics of the power system design. In the upper left hand corner of Figure 32 you will note that the assumed energy converter, its fuel, fuel conversion efficiency and the fuel's heating value are defined. In addition, because several different EOC designs were incorporated into this model the unloader (EOC) design status is identified. In this case, the "TARGET" EOC unit has been used.

Continuing down Figure 32 the top two parameters listed are the net power output from the stationary power system and the design endurance. In this case, these are 1000 watts and 60 days, respectively. Next, there are a number of gill parameters listed. These include details about the oxygen and seawater flows, the various dimensions relevant to the gill design, and important parameters in determining the gill drag and accompanying water pumping power requirements. Interesting parameters among these include the total seawater flow of 1800 lpm providing only 2.8 lpm of oxygen or only 25.9% of the total oxygen available. The gill frontal area is 1 m2. The gill is assumed to be a "box" shape with one side of square cross-section, i.e. the side the water enters from, and the other dimension is listed under tube depth which in this case is 4.8 cm. The total surface area of the tubes for this stationary power system is 247 m2, and the pump motor output power to turn the gear box, propeller and drive the water through the gill is only 3.3 Watts. The water velocity at the gill intake is only 3 cm/sec. It is likely that such a water velocity could be found at the ocean bottom in many of the world's oceans just as a background current. Thus, no seawater pumping would be necessary to run this unit.

Further down Figure 32, there is a list of several EOC parameters. EOC unit power is 25 W/lpm, and the total carrier flow is 2.775 lpm. The total oxygen extracted over the 60 days of operation of this stationary power system equals 330 kg or approximately 20% of the total system weight. It has been noted in past analysis, and it is intuitively obvious that the closer this total oxygen extracted value is to the total system weight, the more attractive the gill/EOC technology becomes for power systems.

For some energy converters, certain waste products are produced, such as CO_2 and water, and a space has been provided in Figure 32 to detail these flow rates. Finally under fuel, the total stored fuel, not including any storage vessels, is tabulated along with the daily fuel consumption rate.

ELTECH Aluminum FC 1.55 V 85 % EFF. 20-Jul-88
ALUM - Incl. w/FC 6130 WATT-HR/KG
CO2 Pump UNLOADER STATUS = TARGET

STATIONARY POWER SYSTEM - CHARACTERISTICS

NET POWER OUT	1092	watts
ENDURANCE	60	days
Gill:		
OXYGEN FLOW	2.882	L/MIN
SEAWATER FLOW	1882	L/MIN
OXYGEN REMOVED FROM SEAWATER	25.9%	
PERMEABILITY	0.00:1	L/SEC/M^2/ATM
GILL FRONTAL AREA (square cross-section)	1	M^2
TUBE DEPTH	0.048	M
SURFACE AREA OF TUBES	247.1	M^2
WATER VELOCITY AT GILL INTAKE	0.03	M/SEC
REYNOLDS NUMBER OF GILL FIBERS	5.031	
GILL TUBES DRAG COEFFICIENT	3.356	
PUMP MOTOR POWER (output shaft)	3.335	WATTS
EDC:		
EDC UNIT POWER	25	W/L2M
TOTAL CARRIER FLOW	2.775	L/MIN
TOTAL O2 EXTRACTED	333.6	KG
Waste Disposal:		
CO2 PRODUCED	0.03	L/MIN
WATER PRODUCED	0.0002	L/MIN
Fuel:		
STORED FUEL	437.43	KG
FUEL CONSUMPTION RATE	7.292	KG/DAY

WEIGHT, VOLUME AND ENERGY BALANCE

Subsystem	Dry Wt kg	%	Disp kg	Net Wt kg	Struct.Vol liters	%	Power watts	%	
ELTECH Aluminum FC	1153	70	829	343	1184	66	1221	100	3
Output Power	0	0	0	0	0	0	1020	83.3	3.822
Gill & Structure	103	6	86	17	103	6	2	0.2	.
EDC & Unloader	162	11	132	30	161	9	70	5.6	60
Carrier Pump	4	0	3	1	4	2	3	0.3	
Motor (Seawater Pump)	42	2	4	29	4	0	2	0.2	
Gears (Seawater Pump)	21	1	9	12	12	1	0	0.0	
Propeller(Seawater Pump)	34	2	17	16	0	0	0	0.0	
Controls	826	2	26	-19	45	3	50	4.2	
Batteries	39	2	17	23	24	1	10	0.9	
Oxygen Storage	39	2	186	-147	826	13	0	0.0	
CO2 Pump	0	0	0	0	0	0	0	0.0	
Waste Heat	25	2	15	10	25	1	0	0.0	
Misc. Pumping	0	0	0	0	0	0	60	5.0	
Fuel - ALUM - Incl. w/FC	0	0	0	0	0	0	0	0.0	
Load	0	0	0	0	0	0	0	0	
TOTALS	1657		1323	334	1763		0		

Figure 32

At the bottom of Figure 32 is a weight, volume and energy balance for all of the various components included in the stationary power system design. This is self explanatory with the component dry weight, displaced seawater volume, wet weight, structural volume and power consumed or produced tabulated in separate columns. For most energy converter systems, the fuel and energy converter weights are separated. However, for the aluminum fuel cells it was most convenient to combine these two systems into one. Noteworthy items to mention about this weight and volume balance is the relatively small portion of the total system occupied by the gill and structure and the EOC and unloader systems. These two systems combined make up only 17% of the power system's weight and 15% of its structural volume. The largest contributor to the weight and volume of the system is the Eltech aluminum fuel cell and the aluminum fuel.

The figures that follow are the results from the most recent analysis of the O_2 extraction technology utilized in a stationary power system configuration. Figures 33 and 34 make up the energy converter comparison - focused on determining which energy converter makes the best overall high energy density package when coupled with the gill/EOC technology. Figures 35 and 36 compare the best converter/O_2 extraction power system to alternative competing power systems. Finally, Figures 37 and 38 test Aquanautics assumptions regarding the EOC design parameters and give an indication of the effects of EOC development on overall power system performance.

CONVERTER COMPARISON/STATIONARY POWER

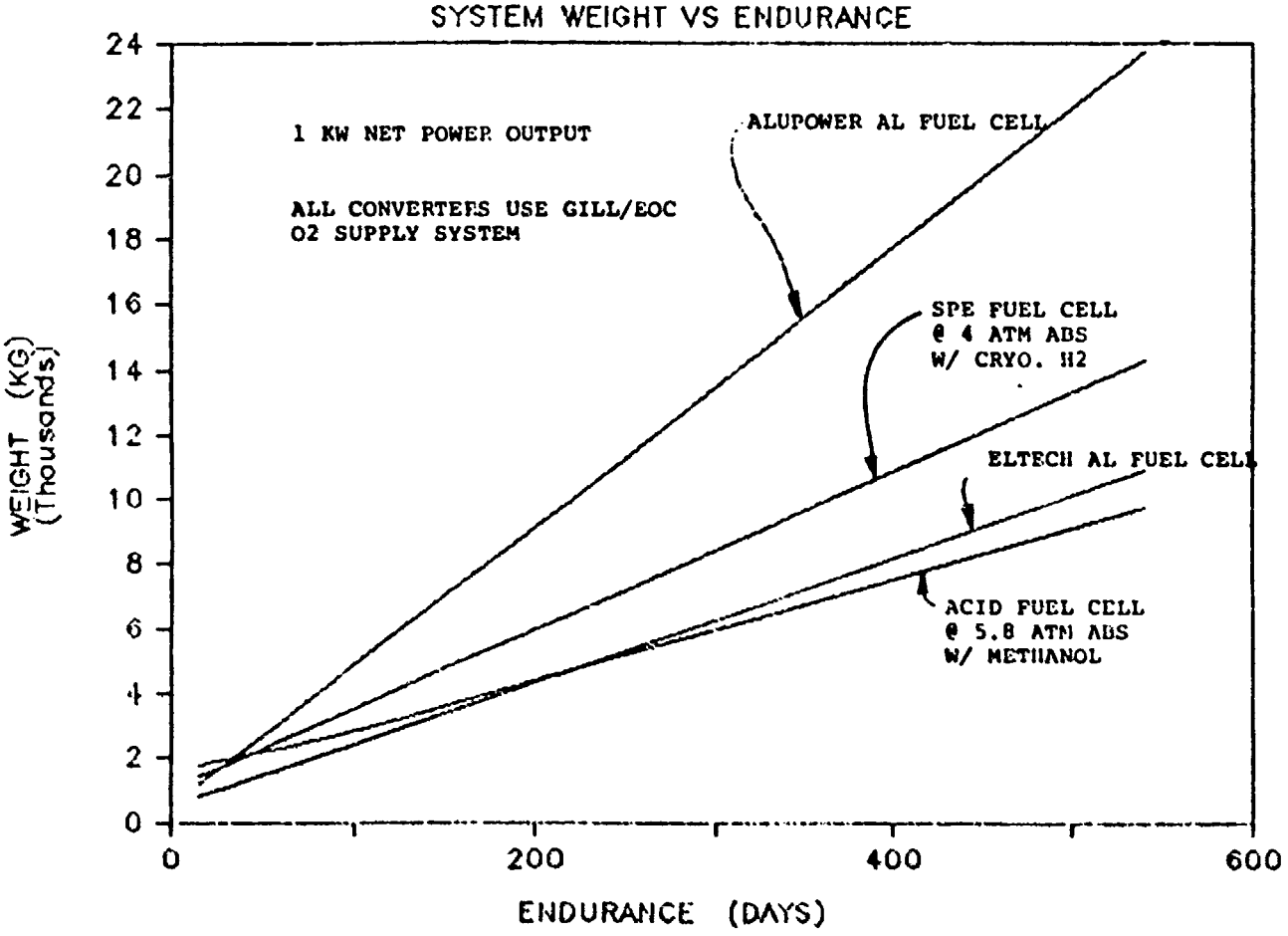

Figure 33

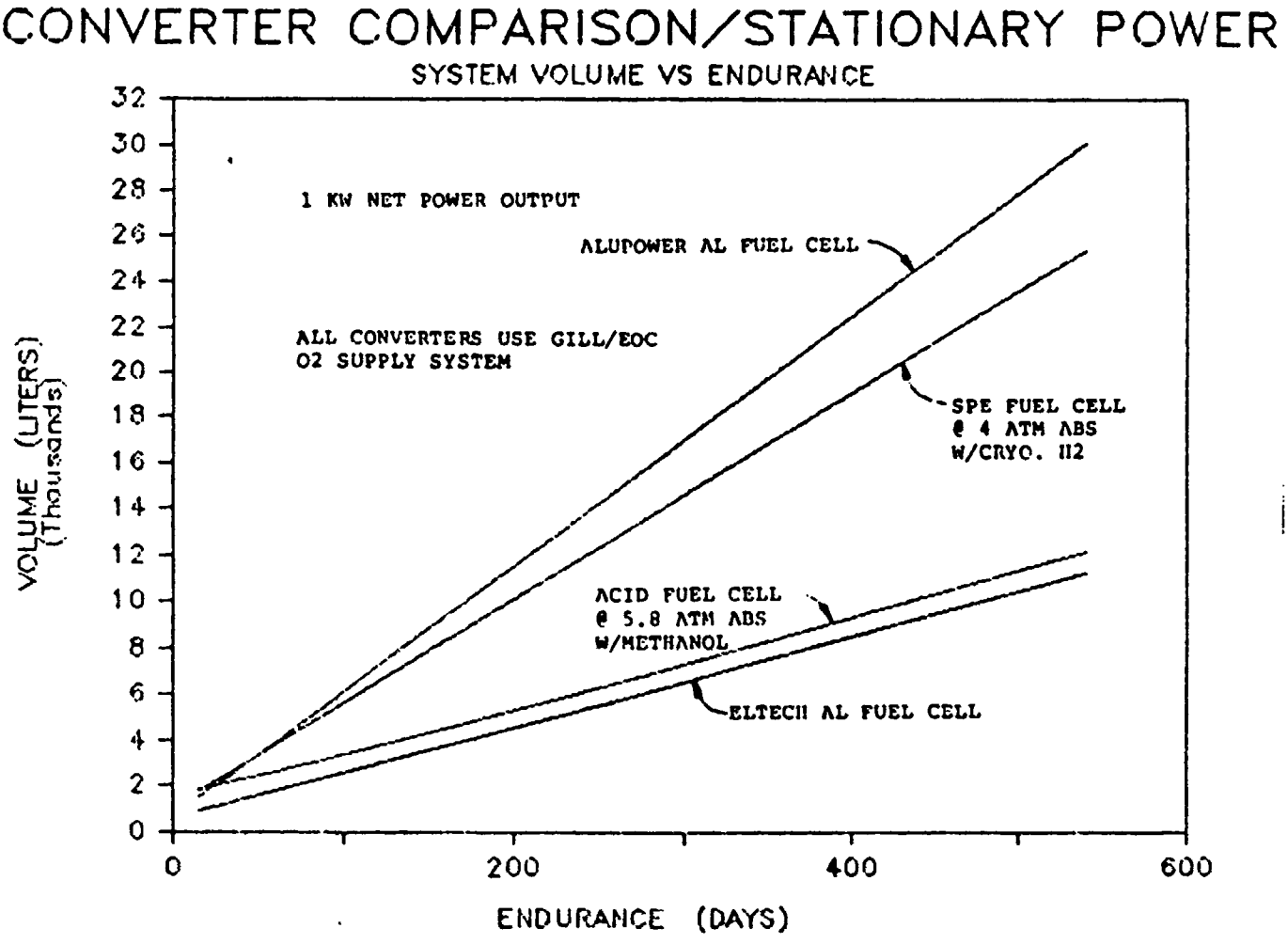

Figure 34

In Figures 33 and 34 a comparison on a weight and volume basis respectively has been conducted of several fuel cells coupled with the O_2 extraction technology. Looking first at Figure 33 note that the comparison is based on a 1 KW net power output and that system weight in thousands of kilograms is plotted on the vertical axis versus endurance in days on the horizontal axis. All subsequent plots that make up this analysis share these features with the substitution of volume in thousand of liters as the vertical axis scale when appropriate.

Figure 33 results indicate that the top ranked energy converter for use with the EOC technology is dependent upon the intended endurance of the stationary power system application. For applications requiring endurances of less than 220 days the Eltech Al-O_2 fuel cell would provide the lowest weight alternative, greater than 220 days the acid fuel cell utilizing reformed

methanol is preferable. However, checking Figure 34, the Eltech fuel cell is best overall converter selection based on a volume analysis. Interestingly, at very low endurances the other competitors, the Alupower Al-O_2 fuel cell and the SPE system, would be second and third choices respectively. The reason for all these intersection points is the fundamental difference between a long endurance system where the fuel and fuel storage medium determine the energy density of the system and a short endurance power unit where the effects of the converter size and weight are more important to the analysis.

For the remainder of this analysis the Eltech Al-O_2 fuel cell is used as the selected "baseline" converter system. This selection is based both on the results from Figures 33 and 34 and on Aquanautics practical experience with this converter system. In the final analysis it may turn out that an SPE fuel cell that can run with reformed methanol will become available, thus eliminating the weight and volume penalty associated with the cryogenic H_2 fuel it uses in this analysis. This development would make the SPE system very competitive with the Eltech Al-O_2 fuel cell and the acid fuel cell using methanol. Another possibility is the improvement of the Alupower Al-O_2 system utilizing seawater as an electrolyte. This fuel cell has many advantages over the alkaline electrolyte system of Eltech, but needs further engineering development to become competitive.

Aquanautics will not eliminate any of these converter systems prematurely for the eventual development of a sea floor stationary power plant or any other application.

Figures 35 and 36 compare the O_2 extraction system coupled with an Eltech aluminum-O_2 fuel cell to several competing technologies. Figure 35 plots total power system dry weight versus endurance, and Figure 36 looks at power system volume versus endurance. Both of these plots illustrate that the O_2 extraction system coupled with an advanced Al-O_2 fuel cell system forms the best power system option of those considered. In addition, it looks increasingly superior to the competition as the mission endurance increases.

STATIONARY POWER SYSTEM COMPARISON

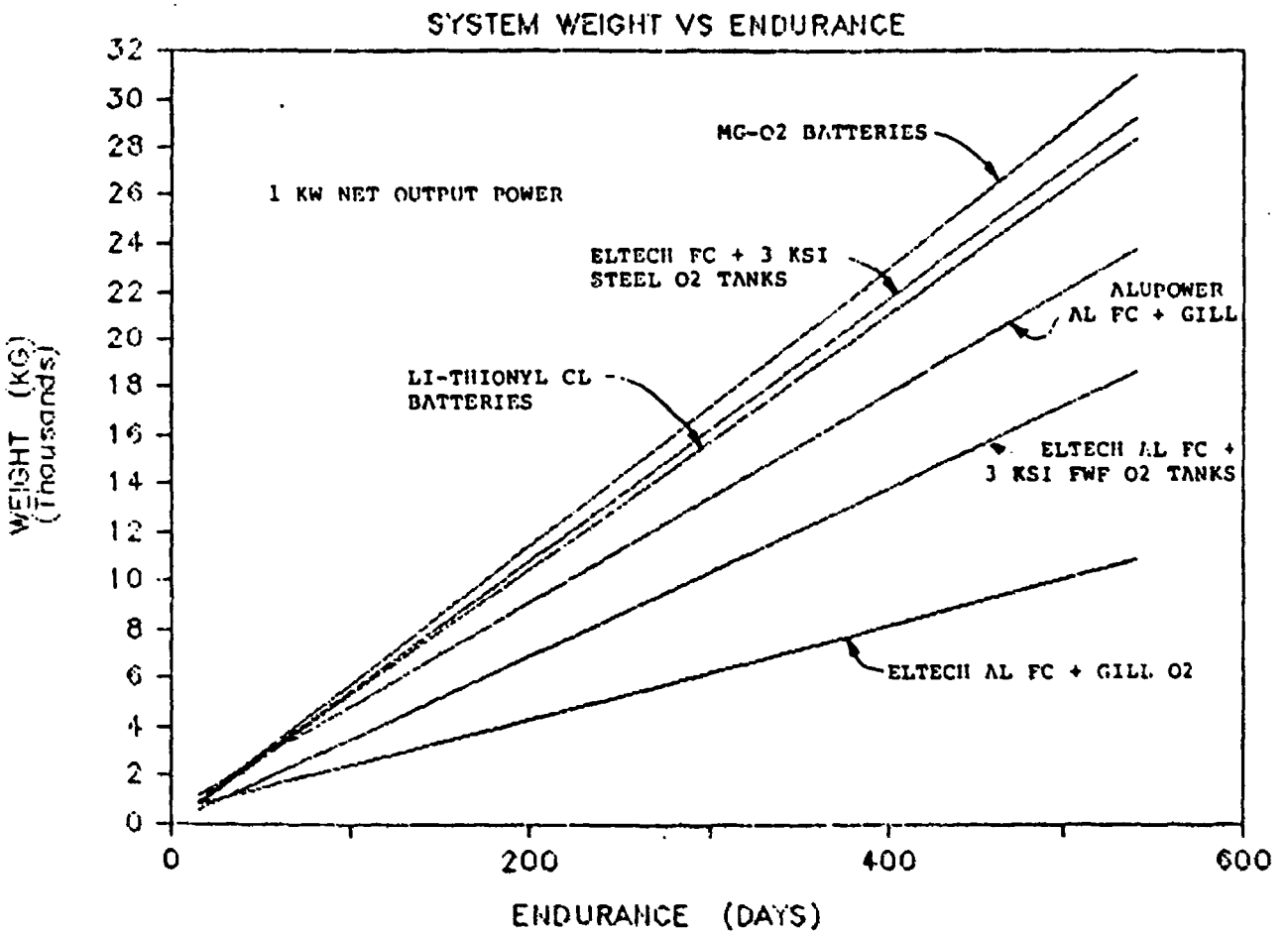

Figure 35

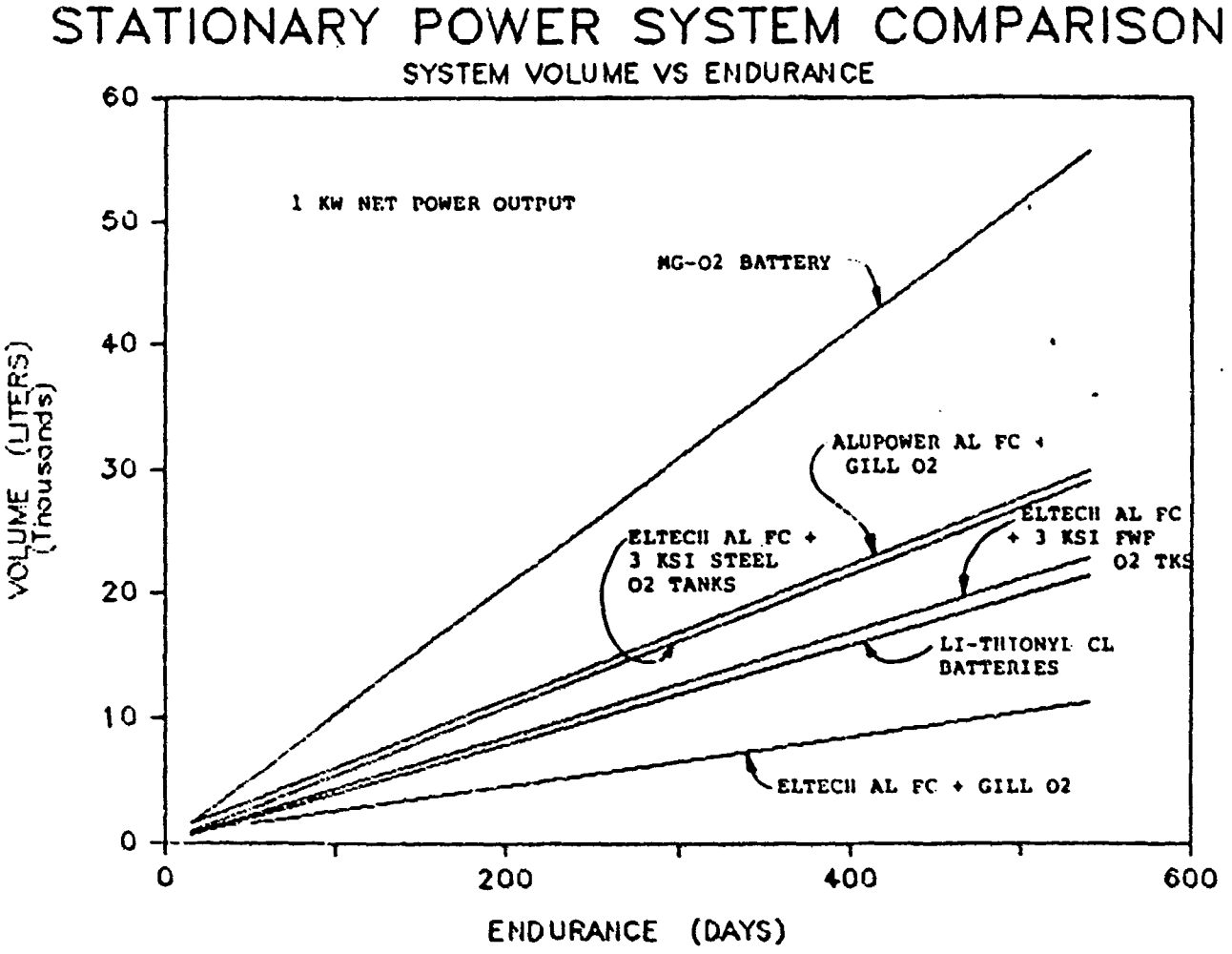

Figure 36

In low endurance missions which may be defined as missions of less than 100 day durations the O_2 extraction system's competitive edge diminishes relative to its nearest competitor - the Al-O_2 fuel cell utilizing O_2 stored in 3 ksi FWF tanks in Figure 35 and also the Li/thionyl chloride battery in Figure 36. At extremely low duration missions (30 days or less), it appears that the 3 ksi FWF O_2 storage option overtakes the gill/EOC supplied power unit on a weight basis, and both the Li/thionyl chloride battery and the FWF stored O_2 system overtake the gill/EOC system on a volume basis.

It is interesting to note that the Mg-O_2 seawater battery is the poorest performing competitor both on a weight basis, and the relative bulkiness of its design further separates it from the pack when analyzed on a volume basis. For similar reasons the Alupower Al-O_2 battery switches from the third ranked competitor when viewed on a weight basis to the fifth ranked competitor on a volume basis. The high density Li/thionyl chloride battery makes an opposite

shift when viewed on a volume basis. These results are skewed somewhat as the stationary power systems which were negatively buoyant were not penalized by the addition of syntactic form in this model. However, buoyant systems did have lead added to their system weight to foam a neutrally buoyant power system.

Most recently, we have received information about H_2 generation by reacting seawater with aluminum. This system has been described in Section 4A. The weight and volume comparisons of using this system are given in Figures 37 and 38.

It is to be noted that although the weight of the system does not improve much, the volume is reduced considerably.

Five different characteristics are plotted on Figures 39 and 40. Each characteristic represents a different level of development of the EOC/gill technology and the resulting performance when coupled with an Eltech Al-O_2 fuel cell. For the other plots already discussed, the EOC development level called "Target Future" was assumed.

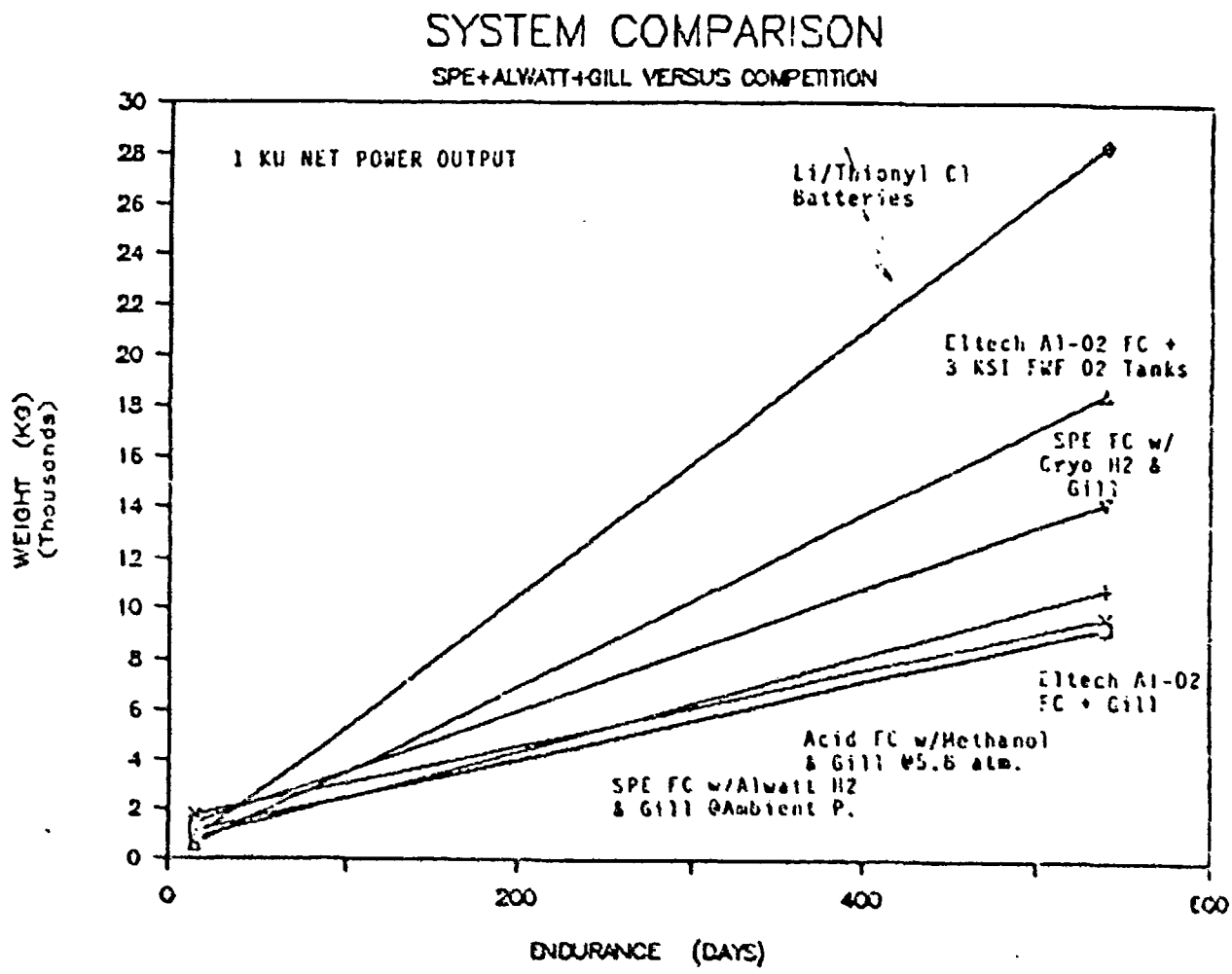

Figure 37

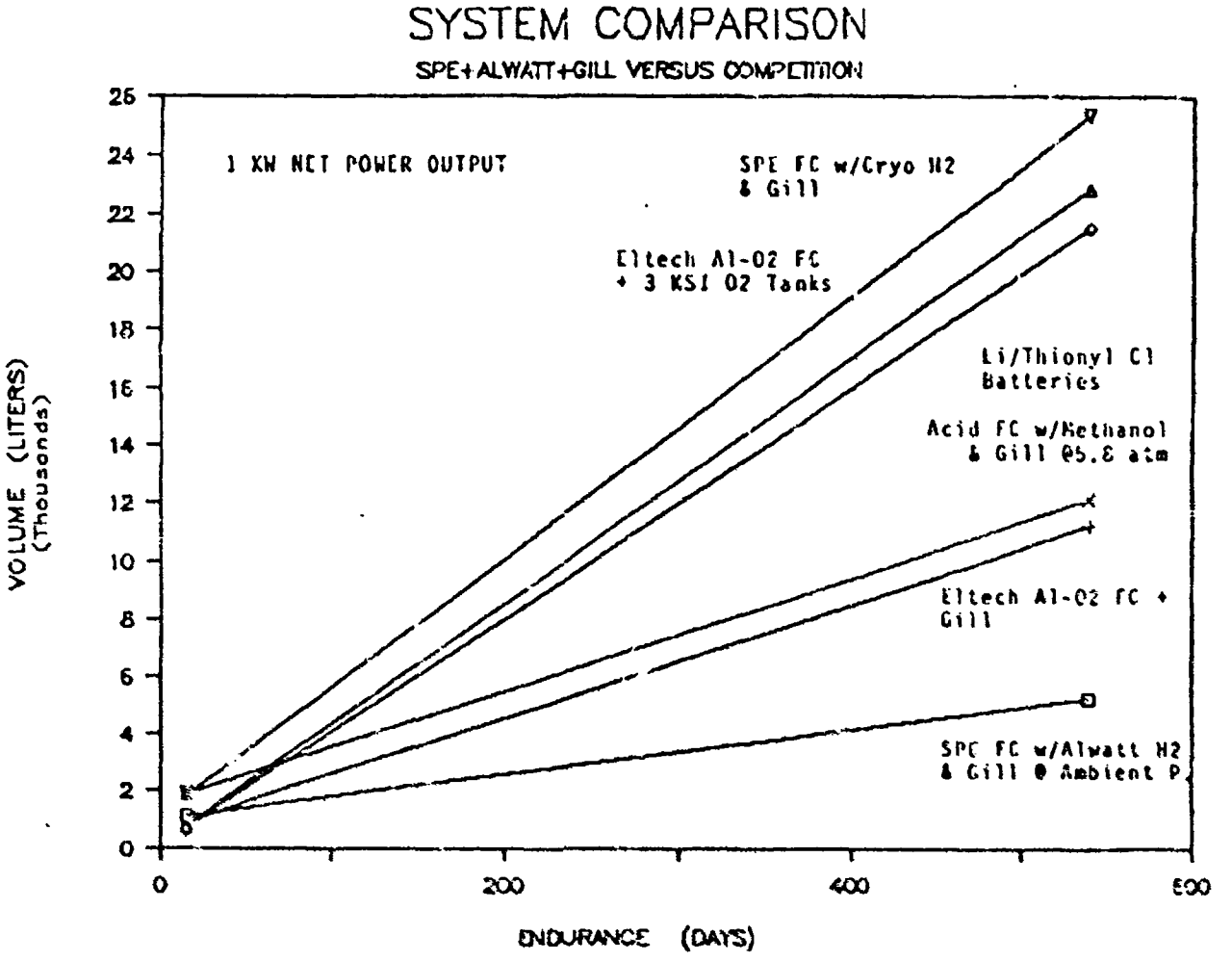

Figure 38

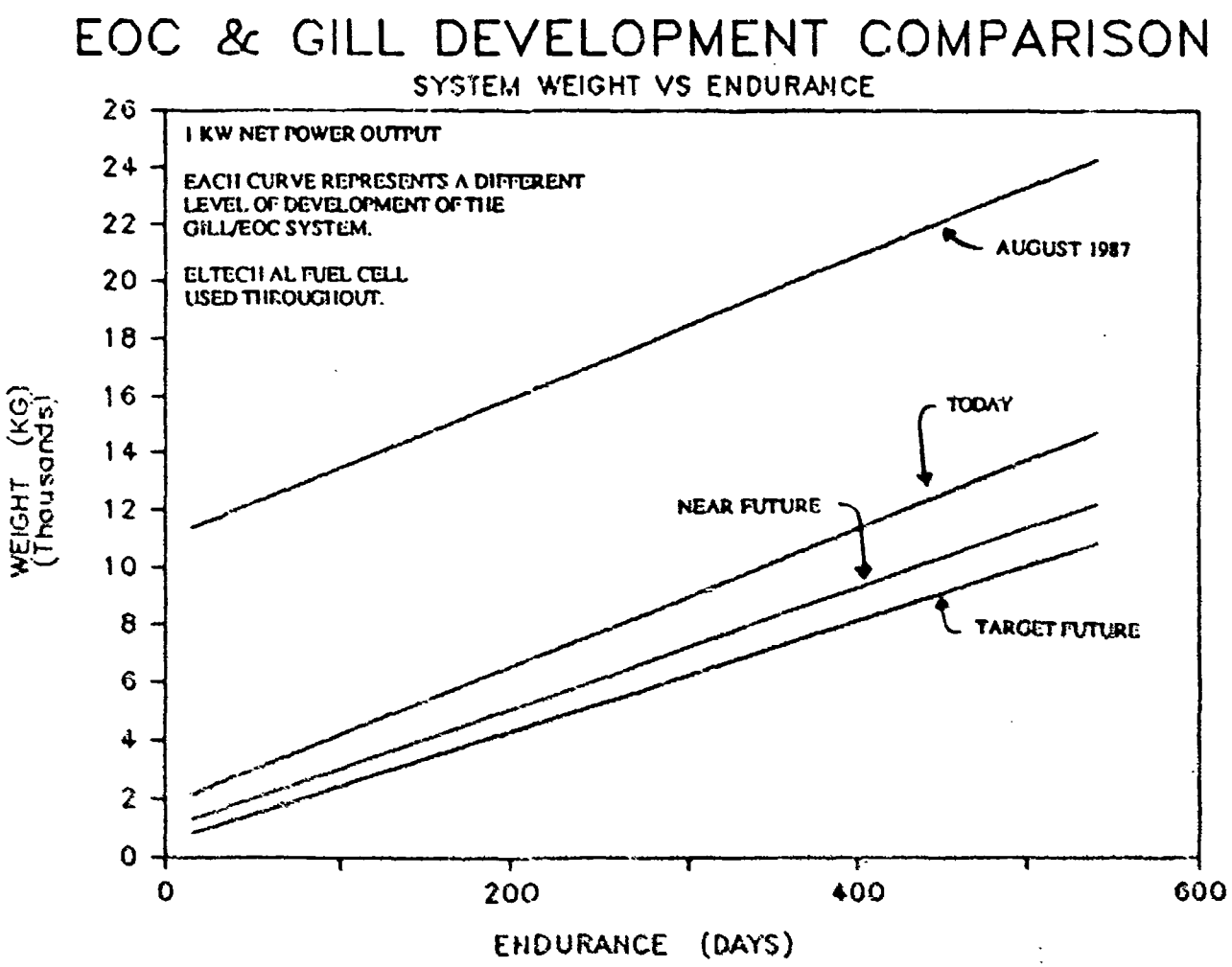
EOC & GILL DEVELOPMENT COMPARISON
SYSTEM WEIGHT VS ENDURANCE
1 KW NET POWER OUTPUT
EACH CURVE REPRESENTS A DIFFERENT LEVEL OF DEVELOPMENT OF THE GILL/EOC SYSTEM.
ELTECH AL FUEL CELL USED THROUGHOUT.
AUGUST 1987
TODAY
NEAR FUTURE
TARGET FUTURE
WEIGHT (KG) (Thousands)
26
24
22
20
18
16
14
12
10
8
6
4
2
0
0
200
400
600
ENDURANCE (DAYS)

Figure 39

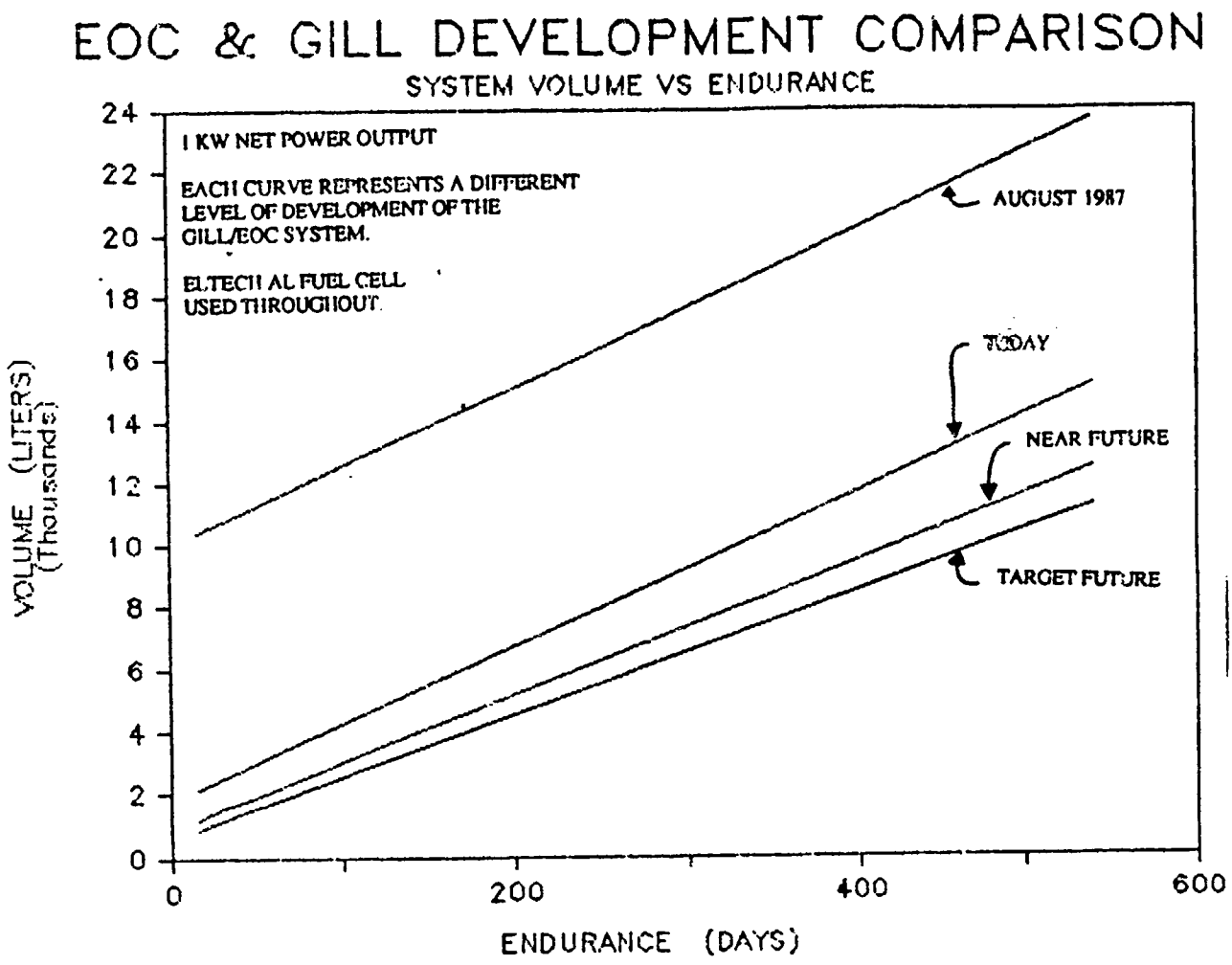

Figure 40

The characteristics in Figures 39 and 40 indicate several things: First, Aquanautics has made a major improvement in their technology between "August 1987" and "today". Second, Aquanautics anticipates another major improvement in the "Near Future" which will have a further positive impact on the overall stationary power system energy density. Finally, even if the "Target Future" level of EOC development is not achieved, by comparison of the "Near Future" curve with the previous plots of competing power systems, it is clear that the oxygen extraction/energy converter will still have a significant advantage over its nearest competitors.

Figure 41 concludes the comparison of the various levels of EOC development. In Figure 41 the weight and volumes of the EOC + gill components for each of the levels of development are compared. Also a theoretical gill + EOC has been added to the list. This table re-emphasizes the advances Aquanautics has made in the development of their electrochemical oxygen cell, and it illustrates that there will still be a large margin between our "Target" EOC development and the Theoretical Minimum.

GILL + EOC WEIGHTS & VOLUMES AT VARIOUS LEVELS OF DEVELOPMENT

DEV. LEVEL	VOL (L)	WT (KG)
THEO.	53	26
TARGET	264	285
NEAR	736	559
TODAY	1563	1471
PAST	10802	9693

Figure 41

To conclude this discussion of the oxygen extraction systems place in the marine power system world, it is instructive to look at the energy map in Figure 24. This graph plots power versus endurance and the niches filled by nuclear power and battery power are well defined. There exists a gap between nuclear systems at high power levels and long endurances and battery systems filling the opposite extreme. The oxygen extraction system coupled with a high energy density energy converter well fills this gap both for stationary and moving vehicle applications in the low to moderate power levels and moderate to long endurance levels.

5C. GILL

To find a membrane for use in the underwater power source, a package on the needs of the membrane has been put together. A list of names from Dr. Cussler and from Bruce Zenner has also been compiled.

These people will be contacted in the second week of October.

A form letter has also been sent out to various membrane companies. The response has been light, with all those responding only selling microporous membranes.

A sample of a solid membrane has been acquired from Membrane Technologies Research. This will be tested for oxygen flux by the end of October. The contact at MTR is Dr. Carl-Martin Bell.

The conceptual design has been made for a membrane test bed. This test bed can be made in-house at a cost of under a hundred dollars a done day's time. It will be completed by the middle of October.

Status:

Work is continuing and will be ongoing at least through the next quarter.

Plan for Next Quarter:

Continue developing contacts for membrane sources and test potential membrane for integrity and oxygen flux.

5D. CONCLUSION

Work is progressing in the direction of designing of the power system for ocean floor use. The system is intended for operation at ambient pressure. A Phase I SBIR project contract has also been awarded to investigate the feasibility of direct feed of the carrier into the fuel cell. This project will complement our power source design.

A model to describe the cell's performance is being developed.

Scaling up of the Aquanautics cell design is also being pursued.

6. APPENDIX

Derivation of Carrier Performance Goals for DARPA Demonstration
(For nomenclature, see end of this section)

The excess power, P, for propulsion etc. is:

$$P = (E_f - E_e - E_C - E_S)Q \tag{1}$$

where Q is the oxygen flow through the extraction system consumed by the fuel cell. E_f, E_e, E_C and E_S are specific powers the fuel cell, the electrochemical oxygen cell, the carrier pump and the sea water pump. Losses for the gas blower, electrolyte pump for the fuel cell, controllers, etc. are lumped into the excess power required as they are either of relatively small magnitude or insensitive to Q.

Solving (1), E_e, the specific power (w.min/l) for the electrochemical oxygen cell is given by:

$$E_e = E_f - E_C - E_S - \frac{P}{Q} \tag{2}$$

Linear approximations which show an excellent fit to experimental data for E_f, E_C, E_S are:

$$E_f = E_f^o - e_f Q \tag{3}$$

$$E_S = E_S^o \tag{4}$$

$$E_C = E_C^o + e_C Q \tag{5}$$

Note that

$$Q = qA_e \tag{6}$$

where q is the oxygen output per unit area for the EOC and A_e is the area of the electrochemical cell. Substituting (3, 4, 5, 6) into (2) gives:

$$E_e = (E_f^o - E_C^o - E_S^o) - (e_f + e_C)\, qAe - \frac{P}{qAe} \tag{7}$$

E_f^o and e_f are determined from voltage and current density data supplied by Eltech for the alloy shown in their proposal, and a 9 cell (yielding approximately 13V), 0.153 m^2 stack. E_S^o was determined from several iterations of Mr. Jensen's parametric model to be $12.5/\eta_S$, where η_S is the seawater pump efficiency.

E_c° and e_c are derived based on several assumptions:

a) The number of gill cartridges required per liter per min. of oxygen is a constant, determined from several iterations of Mr. Jensen's model to be 70 carts/liter per min.

b) The total carrier flow rate will be the minimum flow rate per cartridge required for adequate loading (150 ml/min) multiplied by the number of cartridges. Any carrier flow in excess of this minimum must be included in E_c.

c) The head vs. flow relationship for the MP cell is linear in the range of interest and given by $H^\circ_{cell} + h\frac{Qc}{Ae}$ where Qc is the total carrier flow and H° and h are empirically determined.

From a) and b) the relationship between Q and Q_c can be seen to be $70Q\,(0.15) = Q_c$ or $\frac{Qc}{Q} = 10.5 = k$.

At 150 ml/min the head loss through a gill cartridge is 0.178 m H_2O

Let this quantity be denoted by the symbol H°_{cart}

The carrier pumping cost will be (neglecting plumbing):

$$(E_c^\circ + e_c Q)\,Q = \left(\frac{H^\circ_{cart} + H^\circ_{cell} + h\frac{Qc}{Ae}}{6\eta_c}\right) Qc$$

$$= \left(\frac{H^\circ_{cart} + H^\circ_{cell}}{6\eta_c}\,k + \frac{h(k)^2}{6A_e\eta_c}Q\right)Q$$

Therefore: $E_c^\circ = \frac{(H^\circ_{cart} + H^\circ_{cell})\,(k)}{6\eta_c}$ and

$$e_c = \frac{h(k)^2}{6A_e\eta_c}$$

where η_c is the efficiency of the carrier pump. The attached chart shows a plot of E_c versus q for several values of A_e. The following values were used in calculating this chart:

Fuel Cell Output

$$E_f^\circ = 428 \frac{\text{watt.min.}}{\text{liter}} = 261 \frac{\text{amps·min}}{\text{liter}} \quad (1.64 \text{ volts})$$

$$e_f = \frac{5.38}{A_f} \frac{\text{watt.min}^2\text{m}^2}{\text{m}^2.\text{liter}^2}$$

$$A_f = 0.153 \text{ m}^2$$

Seawater Pumping

$$E_s^\circ = \frac{12.5}{\eta_s} \frac{\text{watt.min}}{\text{liter}}$$

$$\eta_s = 0.21$$

Carrier Pumping

$$k = \frac{Q_c}{Q} = 70 \text{ carts.min.liter}^{-1} \text{ X } (0.15 \text{ liter} \cdot \text{min}^{-1} \cdot \text{cart}^{-1}) = 10.5$$

H°_{cart} = 0.178 m H_2O (@ 0.15 liter/min) from Makai

$\eta_c = 0.10$

for $q > 2$ liter · $\text{min}^{-1}\text{m}^{-2}$, from Aquanautics experiment number 3CB29

H°_{cell} = -0.138 m H_2O

$h = .0728$ m H_2O · liter^{-1} · min · m^2

Nomenclature:

A_e	Membrane area of the oxygen separation electrochemical cell, meter^2.
A_f	Area of the fuel cell,meter^2.
E_c	Normalized power consumed by the carrier pump, watt X minutes X liter^{-1} of oxygen output.
e_c	Incremental carrier pumping cost per unit increase of oxygen output flow rate, watt X minutes^2 X liter^{-2} of oxygen output.
E_c°	Effective fixed normalized power consumed by the carrier pump, watt X minutes X liter^{-1}
E_e	Normalized power consumed by the electrochemical oxygen separation cell, watt X minute X liter^{-1} of oxygen output.

E_f	Normalized power produced by the fuel cell, watt X minute X liter $^{-1}$ of oxygen consumed.
e_f	Incremental power produced by the fuel cell per increase in flow rate of oxygen consumed, watt X minutes^2 X liter^{-2} .
E_f^o	Effective fixed normalized power output of the fuel cell, watt X minute X liter $^{-1}$ of oxygen consumed.
E_s	Normalized power consumed by the seawater pump, watts X minute X liter^{-1} of oxygen output.
E_s^o	Effective fixed normalized power consumption of the seawater pump, watt X minute X liter $^{-1}$
h	Incremental increase in carrier pumping head per unit increase of carrier flow rate, meters X minute X liter^{-1} of carrier flow.
H^o_{cart}	Effective fixed carrier pumping head due to the loader cartridges, meter X minute X liter^{-1} of carrier flow rate.
H^o_{cell}	Effective fixed carrier pumping head due to the oxygen extractor electrochemical cell, meter X minute X liter^{-1} of carrier flow.
η_c	"Wire to water" efficiency of the carrier pump and motor.
η_s	"Wire to water" efficiency of the seawater pump and motor.
k	Volumetric ratio of carrier flow rate to oxygen output.
P	Usable system power output, watts.
Q	Flow rate of oxygen output from the oxygen extraction cell, liters X minute^{-1}.
q	Oxygen output per unit area of electrochemical cell, liter X minute^{-1} X meter^{-2}.
Qc	Carrier flow rate, liter X minute^{-1}.